Influence of Sulphide on the Degradation Pathways for Chlorinated Ethenes

by

Lorretta D. Pinder

A thesis
presented to the University of Waterloo
in fulfillment of the
thesis requirement for the degree of
Master of Science
in
Earth Sciences

Waterloo, Ontario, Canada, 2007

Author's Declaration

I hereby declare that I am the sole author of this thesis. This is a true copy of the thesis, including any required final revisions, as accepted by my examiners.

I understand that my thesis may be made electronically available to the public.

Lorretta D. Pinder

Abstract

Although iron-based permeable reactive barriers are gaining importance in the treatment of groundwater contaminants, there have been field observations indicating that sulphide may affect the degradation rates of certain chlorinated ethenes. Previous observations suggest that sulphide has little effect on TCE degradation rates but can cause a significant decline in the rate of degradation of *cis*-DCE. This study was conducted to systematically test the effects of S^{2-} on TCE, *cis*-DCE, *trans*-DCE, 1,1-DCE and VC. Two different concentrations of sulphide (5 and 50 mg/L) were used in the column experiments. The results showed that the rate of TCE degradation was only slightly reduce in the presence of sulphide, while there was substantial reduction in the rates of degradation of *cis*-DCE, 1,1-DCE and VC. *Trans*-DCE was affected by sulphide, however, not as severely as *cis*-DCE, 1,1-DCE and VC. Raman Spectra showed the presence of a small amount of sulphide precipitates, and corrosion potential measurements showed that sulphide shifted the corrosion potential of the iron to less negative values by approximately 70 mV, suggesting that the change in corrosion potential was not responsible for the preferential degradation of TCE relative *cis*-DCE and VC.

The dominant pathway for TCE degradation is β-elimination, while that for *cis*-DCE and VC is generally considered to be hydrogenolysis, though there is also evidence in the literature indicating that *cis*-DCE and VC can also degrade by catalytic hydrogenation. The results indicate that sulphide does not inhibit β-elimination but severely limits the hydrogenolysis/catalytic hydrogenation pathway. The fact that sulphide inhibited the conversion of ethene to ethane, a known catalytic reaction, indicated that sulphide is acting as a catalyst poison. It is therefore concluded that the primary mechanism for the transformation of *cis*-DCE to VC and for VC to ethene is catalytic hydrogenation, and that sulphide inhibits these transformations through its role as a catalyst poison.

Acknowledgements

Dedication

This thesis is dedicated to my mom – just because I love you!

Table of Contents

List of Tables

List of Figures

Chapter 1
Introduction

1.1 Motivation

In recent years, permeable reactive barriers (PRBs) containing granular iron have become a widely accepted method for *in situ* remediation of groundwater contaminated with chlorinated organic compounds (Kohn et al., 2003, Li and Farrell, 2001). Granular iron can transform contaminants such as tetrachloroethene (PCE), trichloroethene (TCE), *cis*-1,2-dichloroethene (*cis*-DCE), *trans*-1,2-dichloroethene (*trans*-DCE), 1,1-dichloroethene (1,1-DCE) and vinyl chloride (VC) into ethene and ethane as final products (Arnold and Roberts, 2000, Ebert et al., 2006). The transformation process involves redox reactions where the iron metal is oxidized and the organic compound is reduced. Iron metal is a reductant with a standard reduction potential of -0.440 V (Matheson and Tratnyek, 1994).

PCE and TCE are commonly found as groundwater contaminants and can be effectively treated by iron. However, if the transformation process is not complete, then the lesser-chlorinated ethenes such as *cis*-DCE and VC can remain in the groundwater. It has alo been found that less chlorinated ethenes such as *cis*-DCE and VC degrade more slowly than the more chlorinated parent compounds. These intermediates are themselves suspected human carcinogens and are regulated in drinking water (Butler and Hayes, 1998). To ensure that the transformation process is completed, the PRB must be carefully designed to provide a sufficient residence time. Most often column experiments are performed with the site water to determine reaction rates for the purpose of designing the PRB. Column tests can also assist in identifying groundwater constituents that may inhibit the ability of the granular iron to degrade the contaminants.

One such groundwater constituent that may affect the performance of a granular iron PRB is sulphide. Some laboratory tests have shown that sulphide can accelerate degradation (Hansson et al., 2006) while others have shown inhibiting effects (Ebert et al., 2006). Ebert et al. (2006) tested the degradation of several chlorinated ethenes from various field sites. At one site in particular there was a low reactivity for *cis*-DCE while TCE degraded completely at reaction rates comparable to those derived from other column experiments. The authors did not provide an explanation for the apparent inhibition of *cis*-DCE degradation; however, they suspected that the inorganics in the column source

solution, which included sulphate and possibly sulphide, may have interfered with the performance of the granular iron.

In an above ground reactor, TCE was observed to degrade at a similar rate over an extended period of time. However, the rate of degradation of *cis*-DCE declined over the same period of time as indicated by increasing concentrations in the effluent. A significant decline in sulphate was also observed across the reactor (EnvrioMetal Technologies Inc., Personal Communication). These observations led to a laboratory column study that compared the reactivity of iron collected from the field site with the fresh iron that was originally used at the site. It was found that compared to the fresh iron, the half-lives of *cis*-DCE and VC were greatly increased for the reactor material; however, the half-life of TCE was not affected. Raman Spectroscopic analyses indicated significant FeS on iron samples from the reactor. This suggests that sulphide may have a negative effect on the performance of granular iron for the remediation of TCE and its breakdown products. Though various factors are known to affect the performance of granular iron, sulphate/sulphide are unusual in that they do not appear to have a substantial effect on the degradation of TCE but dramatically reduce the degradation rate of the DCEs and VC.

The purpose of this study was to test how sulphide affects the breakdown of TCE, *cis*-DCE, *trans*-DCE, 1,1-DCE and VC by granular iron. An improved understanding of these effects may lead to a better understanding of the consequences of increased sulphide concentrations in groundwater on PRB reactivity towards various organic compounds.

1.2 Sulphur Compounds in the Environment

Sulphur can have multiple oxidation states ranging from +VI to –II, making it both an electron acceptor and donor in redox reactions (Faure, 1998). Major forms of sulphur in the subsurface include sulphate and sulphide minerals, dissolved sulphate (SO_4^{2-}), dissolved sulphide (HS^-) and hydrogen sulphide gas (H_2S) (Langmuir, 1997). Depending upon the Eh and pH, most surfacewater and groundwater contains sulphate. Hydrogen sulphide and HS^- are major species in organic-rich, anaerobic water-logged soils and sediments (Langmuir, 1997).

Sulphate is present in many groundwater systems and can be derived from a variety of sources. Sulphate in groundwater may occur naturally from the dissolution of sulphate minerals, the oxidation

of reduced sulphur minerals, or from a variety of both organic and inorganic atmospheric and soil sources (Moncaster et al., 2000). The sulphate concentration in groundwater can exceed 1000 mg/L, but covers a wide range depending on the local environment (Langmuir, 1997). Even though sulphate has a low toxicity, its presence deteriorates the quality of drinking water. High sulphate concentrations can affect water hardness, cause corrosion in pipelines, and can adversely affect drinking water (Knöller, 2005).

The reduction of sulphate to sulphide occurs under anaerobic conditions in the presence of sulphate-reducing bacteria and a source of organic carbon. Sulphate-reducing bacteria are a diverse group of anaerobes that can use sulphate as an electron acceptor for the oxidation of an organic substrate. One example of bacteria involved in this process is *Desulfovibrio desulfuricans,* which prefers a pH between 6 and 8, but can function between pH 4.2 and 9.9 (Langmuir, 1997). The reduction of sulphate takes place primarily a few centimeters below the water table, but may continue to a depth of several meters, depending on the availability of other more oxidative electron acceptors such as oxygen and nitrate. The sulphide produced by sulphate reduction commonly precipitates with various metal species including ferrous iron (Butler and Hayes, 1998).

1.3 The Degradation of TCE by Granular Iron

Figure 1, which was adapted from Arnold and Roberts (2000) and Li and Farrell (2000), shows the degradation pathways of TCE and its breakdown products by granular iron. TCE can degrade by either reductive β-elimination/hydrogenolysis/catalytic hydrogenation. Reductive β-elimination is the removal of two chlorines with the formation of an additional C-C. Hydrogenolysis is the replacement of a halogen by hydrogen. Arnold and Roberts (2000) showed that 97% of TCE is degraded by reductive β-elimination producing chloroacetylene. The resulting chloroacetylene then undergoes hydrogenolysis to form acetylene, which may then be further reduced to ethene or ethane through catalytic hydrogenation (Arnold and Roberts, 2000 and Li and Farrell, 2000). Catalytic hydrogenation is the reduction of multiple bonds and the addition of hydrogen in the presence of a catalyst. Iron is not known as an effective catalyst; however, the surface of the iron, its defects, or other solid phases occurring in the system could provide the needed catalyst (Matheson and Tratnyek, 1994).

TCE can also degrade by hydrogenolysis to form *trans*-DCE, *cis*-DCE or 1,1-DCE. *Cis*-DCE is the primary product (3%) detected from the degradation of TCE by granular iron through this pathway. (Arnold and Roberts, 2000). *Trans*-DCE and *cis*-DCE can degrade further to acetylene by reductive β-elimination. Arnold and Roberts (2000) proposed that 94% of *cis*-DCE and 99% of *trans*-DCE degrade by reductive β-elimination. Both can also degrade by hydrogenolysis or catalytic hydrogenation to form VC (Arnold and Roberts, 2000, Li and Farrell, 2000). It is believed that 1,1-DCE degrades by either catalytic hydrogenation or reductive α-elimination to form ethene. In all cases, the final products for the degradation of TCE is ethane, formed through the catalytic hydrogenation of ethene. The amounts of each product can vary depending on the properties of the iron, other chemicals in solution, temperature and pH (Farrell et al., 2000).

1.4 Loss of Reactivity

Several studies have investigated the effect of naturally occurring groundwater constituents such as calcium carbonate, nitrate, silica, chromate and natural organic matter on the performance of iron PRBs. Calcium carbonate can negatively affect the performance of iron PRBs by forming carbonate precipitates that reduce the reactivity of the iron (Zhang and Gillham, 2005). These precipitates may also reduce the porosity and permeability. The accumulation of calcium carbonate can thus reduce the rate of TCE degradation, having a negative effect on the long-term performance of iron PRBs.

In the presence of nitrate the TCE reduction rate was significantly decreased due to the oxidizing effect of nitrate (Ritter et al., 2003). At a nitrate concentration of 100 mg/L, the pre-existing passive layer on the iron surface remained. Nitrate also led to a positive shift in corrosion potential, with higher nitrate concentrations resulting in a greater change in the corrosion potential (Lu, 2005). An increase in corrosion potential can lead to thermodynamic conditions that are more favourable for the formation and stability of higher valency iron oxides on the iron surface. These passive oxides act as a physical barrier and greatly interfere with charge transfer processes and thus both TCE and nitrate degradation rates declined. Raman spectroscopic measurements confirmed the presence of passivating iron oxides after nitrate addition (Lu, 2005).

Research has also examined the influence of silica on the degradation of organohalides in granular iron columns since silica has corrosion-inhibiting properties (Kohn and Roberts, 2006). It was found that dissolved silica species could negatively affect the reactivity of iron toward chlorinated solvents.

4

The iron reactivity declined by 65% for TCE, 74% for 1,1,2-trichloroethane and 93% for 1,1,1-trichloroethane. It was suggested that the adsorption of silica species could lead to impaired PRB performance by causing a shift in the product distribution toward less desirable reaction products such as *cis*-DCE and VC (Kohn and Roberts, 2006).

Chromate has also caused TCE degradation rates to decrease by about 50% (Lo et al., 2005). It was observed that the presence of Cr(VI) resulted in a positive shift of the iron corrosion potential (Yang, 2006). The reduction products Cr(III) formed various Fe(III)/Cr(III) baring oxides and a passive oxide film at the iron surface (Jeen, 2005).

1.5 Sulphur and Granular Iron

Farrell et al. (2000) found that in iron columns fed with water containing chloride and sulphate, the effective half-life for TCE dechlorination increased from approximately 400 minutes to approximately 2500 min after 667 days. However, since chloride and sulphate were in the feed solution together, the influence of sulphate alone was not determined.

In columns filled with granular iron, Kober et al. (2002) initially observed that sulphate passed through without significant changes in concentration. However, after 70 pore volumes (PV), it was noted that there was a loss of sulphate. Coincidentally, after 70 PV, the degradation of *cis*-DCE and VC slowed dramatically yet TCE removal was still high. It is thought that a time lag of 70 PV was needed for the bacterial population within the column to be established. However, in this study there was no measurement of sulphide to confirm its presence.

Iron sulphide minerals are common minor constituents of sediments and aquifers that are produced primarily as a result of microbial reduction of sulphate. The prevalence of these minerals, as well as their reactivity, has led several groups of researchers to investigate their ability to reduce contaminants (Carlson et al., 2003, Butler and Hayes, 1999). Fe and FeS are both reactive materials. FeS has been shown to degrade TCE and PCE (Butler and Hayes, 1999). However, there was only a 17% reduction in the concentration of 1,1-DCE after 120 days in the presence of FeS (Butler and Hayes, 1999) compared to complete degradation as seen with Fe (Arnold and Roberts, 2000). When TCE was degraded by FeS, both acetylene and *cis*-DCE were produced. 1,1,1,2-tetrachloroethanes

5

can also be transformed by FeS into TCE, *cis*-DCE and acetylene (Butler and Hayes, 2000). Their results showed that *cis*-DCE was produced in this process but did not further degrade.

Treatment of iron metal with bisulphide has been shown to increase the rate of transformation of TCE, PCE and carbon tetrachloride (CT) (Butler and Hayes, 2001). These authors suggest that iron metal placed in PRBs could, either naturally or through engineered measures, form a FeS coating that would enhance its reactivity with pollutants such as TCE (Butler and Hayes, 2001). They also suggested that encouraging the growth of sulphate-reducing bacteria in the vicinity of iron PRBs could be an effective way to enhance the long-term reactive stability of iron PRBs (Butler and Hayes, 2001). These results seem to contradict many other studies, particularly those considering HS^- as a catalyst poison. However, in these studies, the degradation of *cis*-DCE was not examined in detail. Therefore, further research is needed to determine the effect of sulphide on the degradation of TCE and its degradation products.

Recent studies by Hansson et al. (2007) investigated the influence of sulphide on the degradation kinetics of CT in the presence of very pure iron. It was found that a FeS film is formed in the presence of sulphide which could inhibit the charge transfer and initially slow down the degradation of CT. However, as the film ages it develops cracks and further promotes corrosion and hydrogen embrittlement of the iron, resulting in dissolution fractures and crack formation in the iron, resulting in a higher exposed surface area. This, in turn, increases the rate of degradation for CT. However, the mechanism for the degradation of CT by pure iron is charge transfer (Matheson and Tratnyak, 1994) compared to TCE which degrades mainly through β-elimination (Arnold and Roberts, 2000).

More study is required to determine how sulphide affects the degradation of TCE and its breakdown products by granular iron. Of particular importance, TCE appears to degrade in the presence of sulphide, while *cis*-DCE and VC do not. The reasons for the preferential degradation of TCE compared to *cis*-DCE and VC is particularly interesting.

Based on the literature, it is assumed that within an iron PRB sulphate is bioreduced to sulphide (Ebert, 2006). Consequently, in this study, the effects of sulphide will be focused upon, even though sulphate is the major form of sulphur found at most contaminated sites. It is also hypothesized that

sulphide influences the degradation of TCE such that TCE degrades at a normal rate; while *cis*-DCE and other chlorinated ethenes degrade at a much lower rate.

1.6 Goal and Objectives

The goal of this research was to determine the cause of changes in degradation rates of TCE and its chlorinated degradation products by iron in the presence of sulphide. The specific objectives were to:

1. Determine the effect that sulphide has on the kinetics of degradation of TCE, *cis*-DCE, *trans*-DCE, 1,1-DCE and VC.
2. Determine the concentration effect of sulphide on the rate of degradation of TCE, *cis*-DCE and VC.
3. Determine the effect of sulphide on the corrosion potential of granular iron.
4. Determine the reduction potentials of TCE and *cis*-DCE.
5. Determine whether the degradation pathways and mechanisms are altered by the addition of sulphide for TCE, *cis*-DCE and VC.

Five column experiments were established with different influent solutions to test the effects of sulphide on the degradation of TCE and its degradation products. Three of these were used for determining the kinetics, while the other two were used to examine the effect of sulphide on the corrosion potential. The breakdown products of each contaminant were measured in all columns. Electrochemical experiments were performed to determine the reduction potential of TCE and *cis*-DCE. By comparing the corrosion potentials in the presence and absence of sulphide with the chemical reduction potentials of TCE and *cis*-DCE, the effect of sulphide on the degradation pathways and mechanisms was examined.

Chapter 2

Materials and Methods

2.1 Chemicals and Materials

The granular iron used in the column experiments was obtained from Connelly-GPM, Ltd. (Chicago, IL) and was used as received. TCE (certified ACS) was from Fisher Scientific, DCE isomers and VC were from Sigma-Aldrich and reagent grade sodium sulphide was acquired from Fluka. Mercury, used in the reduction potential measurements, was obtained with a purity of 99.9998% from Johnson & Matthey, and potassium perchlorate was from Sigma-Aldrich.

2.2 Column Experiment

2.2.1 Column Setup

Two sizes of Plexiglas^{TM} columns were used in this project. One was 30 cm long x 2.5 cm I.D> with 15 sampling ports located at 2 cm intervals along the columns (Figure 2). These columns were used to examine the degradation of the chlorinated ethenes at different levels of sulphide (A- Control, B- 5 – mg/L sulphide, C- 50 mg/L sulphide).

The second type, columns D and E (Figure 3), were used to measure the corrosion potential during VOC degradation in the presence of sulphide. These were similar to the first type but each was 20 cm in length and 3.8 cm I.D. In addition to the regular sampling ports located at 2.5, 5, 10, 15 and 17.5 cm from the influent end, two additional ports were installed to hold the reference electrodes at 5 and 15 cm from the inlet. A pure iron rod located at the opposite side of the lower reference electrode (5 cm) acted as the electrical connector. A detailed column description for corrosion potential measurements is given in Lu (2005).

All five columns were packed uniformly with 100% granular iron. To ensure a homogeneous packing, similar amounts of iron were added to the columns in depth increments of about 2 cm. After each addition, the iron was gently tapped with a Plexiglas^{TM} rod. For the two columns that had corrosion potential measurements, the reference electrode compartments were added as the column

was being packed. Screens (100-mesh nylon) were used at each end of the column to prevent iron from plugging the influent and effluent tubing.

To ensure complete saturation, each column was flushed with CO_2 for at least 2 hours prior to the addition of deoxygenated Millipore water at a flow rate of approximately 0.8 mL/min. Once the columns were saturated, the chlorinated solvent solution was introduced at a flow rate of approximately 0.2 mL/min. This flow rate was maintained during the experiments, resulting in a residence time of between 6 and 7 hours for the 30 cm long columns and 9 to 10 hours for the 20 cm columns. The larger residence time in the shorter columns was a consequence of a the larger diameter.

2.2.2 Source Solutions

The TCE, *cis*-DCE, VC, *trans*-DCE and 1,1-DCE solutions were prepared by adding concentrated stock solutions in methanol to Millipore water in 5 L carboys. The Millipore water was purged with oxygen-free nitrogen gas for at least two hours prior to the addition of the chlorinated organic compounds. For the solutions containing sulphide, different amounts of sodium sulphide hydrate were added to the carboys containing deoxygenated Millipore water and then mixed with the various organics. The solutions were fed to all columns through a multi-channel peristaltic pump. The effluent from the columns was collected in plastic waste containers.

To prevent oxygen contamination, stainless steel tubing was used to connect the source bottles to the columns, except for a 15 cm length of Viton tubing that passed through the pump. Mylar balloons filled with oxygen-free N_2 were used to supply the headspace as the solution level declined in the source bottles. For all the solutions, the N_2 gas from the balloons first passed through a bottle filled with a solution identical to the source solution before it passed into the source bottles, thus through gas and aqueous phase partition, the concentration in the source bottles remained relatively constant.

The concentrations of organics in the influent solution were 10 mg/L and two sulphide solutions were prepared at 5 mg/L and 50 mg/L by adding Na_2S. For columns A, B and C, the chlorinated organics were added in combination or individually, according to the sequence given in Table 1.

Samples for analysis were collected from the sampling ports and from the influent line using a 1 mL or 5 mL glass syringe, depending upon the analyses to be performed. Stagnant water was discarded from each port prior to sampling. Between samples, the syringes were rinsed three times with methanol, followed by three times with Millipore water.

2.3 Open Circuit Potential

Open circuit potential is the potential naturally adopted by an isolated metal, where the total rate of oxidation is equal to the total rate of reduction. That is, there is no net current, with the flow of electrons in the oxidizing direction equal to the flow of electrons in the reducing direction. Granular iron PRBs are a passive treatment method, and therefore operate under open circuit potential conditions (Ritter, 2000).

The corrosion potential was measured in the columns between the $Ag/AgCl^-/Cl^-$ reference electrode and the iron grains that were in contact with the tip of the glass compartment containing the reference electrodes. The iron grains at the tip of the glass compartment served as the working electrode, and the pure iron rod at the base of the column served as an external electrical connector. One end of the electrical connector rod was in contact with the iron grains at the base of the column, while the other end protruded from the column and was connected to a high input impedance preamplifier, which prevented current flow between the electrodes. The impedance unit was connected to a UPC601-U Universal PC Sensor Interface Card, which transmitted data to a computer. The measured potential values represent the average values for the iron particles in the immediate vicinity of the tip of the glass reference electrode compartment. It is possible that the potentials varied due to the heterogeneity of the iron, and thus the measured corrosion potential was an average value for the area close to the reference electrode. All potential measurements are reported versus the Standard Hydrogen Electrode (SHE).

Since the sulphide in the columns could damage the $Ag/AgCl/Cl^-$ reference electrodes, the measurements were not recorded continuously. Instead, the electrodes were placed in the column for a few hours each time the measurements were being made, then removed and restored in solution.

2.4 Raman Spectroscopic Measurements

At the end of the column operations, iron samples from Columns B and C were examined using Raman spectroscopy. The columns were detached from the source solutions and transferred to a glovebox containing a 100% nitrogen atmosphere, to preserve the iron surfaces during sampling. For Column B (low sulphide) the nylon Swagelok fitting was removed form the side of the column 5 cm above the influent end, so the iron could be accessed and sampled. For column C (high sulphide) the iron was taken from the bottom of the column, at the influent end. A stainless steel spatula was used to remove grains of iron which were transferred to a 5 mL screw cap glass vial, pre-filled with solution taken from the column, and sealed with a Teflon-faced butyl rubber septum. The samples were then stored in the glovebox for two weeks until the analysis could be performed.

A Renishaw 1000 Raman microscopic system was used for ex situ measurements. A 41 mW laser was used, which resulted in approximately 9mW at the observation stage and even less at the sample surface. Such low intensity is unlikely to alter the surface films. The microscope objective lens had a magnification of 50. The resulting laser focus had a diameter of ca. 5 um on a rough surface and a depth of ca. 3 um.

A specially constructed Raman cell was used to contain the iron and prevent alteration of the surface film. Several grains of iron were added to a 5.4 mL glass hypovial that was partially filled with storage water. The Raman cell consisted of the hypovial with a Teflon septum and cap. A TCTFE rod went through the cap of the hypovial. Tightening the rod and the cap, which displaced any excess water, created the cell. The distance between the iron grains and the optically flat surface of the bottom of the hypovial was adjusted by sliding the PCTFE rod up and down.

In order to avoid bias while selecting spots for Raman analysis, iron grains were randomly picked under the microscope. For Column B, 10 different spots were analyzed on the same grain. For column C, 5 different spots were analyzed on each of 2 different grains.

2.5 Reduction Potential Measurements

The reduction potentials of TCE and *cis*-DCE in aqueous solutions were measured using Differential Pulse Voltammetry (DPV). The electrochemical experiment for this study was modified from a

method described elsewhere (Odziemkowski et al., 2000). Mercury was used as an electrode in this study because it has a very high over-potential for hydrogen evolution and is therefore more suitable than other electrode materials to study reduction reactions.

For TCE and *cis*-DCE reduction potential measurements, 1 mL of pure-phase TCE or *cis*-DCE was first injected into the cell. However, it was found that the pure-phase solvent would not dissolve easily and therefore the results were not reproducible. Also, the breakdown products for TCE or *cis*-DCE were hard to detect because if any products were formed, they would dissolve into the undissolved pure phase instead of staying in the aqueous solution. Subsequently TCE or *cis*-DCE methanol stock solution was prepared and injected into the electrochemical cell. This modification facilitated organic dissolution and product analysis.

Samples were taken from the cell after about 2 hours of DPV for analysis of TCE and *cis*-DCE and to determine if breakdown products such as VC and acetylene had formed. Special precautions were taken to ensure that the cell had been cleaned properly and that there was no oxygen in the system.

2.6 Analytical Methods

2.6.1 Organics

Analyses for TCE, DCE isomers, and VC were conducted using a Hewlett Packard 5890 Series II gas chromatograph (GC) equipped with a HNU photoionization detector (PID) with a bulb ionization potential of 10.2 eV. The GC was fitted with a fused silica capillary NSW-PLOT column (15 m 0.53 mm ID). Samples of 1 mL were collected in glass syringes and diluted with 3 mL Millipore water and placed in 10 mL glass vials. The vials were closed with crimp caps with Teflon-lined septa, creating a ratio of 6 mL headspace to 4 mL aqueous sample. The samples were placed on a rotary shaker for 15 min to allow equilbiration between the water and gas phases. The samples were injected into the GC using a Hewlett Packard 7694 headspace auto sampler, with a 1 mL stainless steel sample loop. The samples were placed on the analyzer oven for 2 min at 75°C, and subsequently injected onto the chromatograph. The temperature program increased from 50 to 200°C at 20°C/min, and was held for 7 min. The injector and detector temperatures were 100°C and 120°C, respectively. The carrier gas was helium with a flow rate of 5.5 mL/min. Data was collected with a Pentium 166 computer, using HP-Chemstation Version 5.04.

For hydrocarbon gases, analyses were conducted using an HP 5790 A GC equipped with a flame ionization detector (FID) and a Megabore GS-Q capillary column. A 2.5 mL sample was placed in a 5 mL glass screw-cap vial, sealed with a Teflon-faced sptum, thus creating a solution-to-headspace ratio of 1:1. Samples were placed on a rotary shaker at 300 rpm for 15 min to ensure equilibrium between the water phase and gas phase. For analysis, a 250 uL sample was injected. The GC had an initial temperature of 60°C, which was held for 3 minutes. The temperature was then increased at a rate of 15°C/min reaching a final temperature of 120°C and then was held at that temperature for 10 minutes. The detector temperature was 280°C and the injector temperature was 120°C. The carrier gas was ultra pure nitrogen with a flow rate of 20 mL/min. The gases analysed included ethane and ethene. For acetylene analysis, an isothermal method was used. The GC had a temperature of 40°C, held for 5 minutes. The detector and injector were both set for 200°C. The MDLs for all analyses are given in Table 2.

2.6.2 Inorganics

pH

pH was measured using an Orion 910600 glass combination pH electrode attached to a Markson Model 90 meter. The probe was calibrated each day using commercially prepared pH 7 and pH 10 buffers.

2.6.2.1 Dissolved Oxygen

Dissolved Oxygen concentrations were determined using CHEMetsR Dissolved Oxygen Kits. Kit number K-7501 was suitable for dissolved oxygen concentration in the range of 0.01-1.0 mg/L. The kit used the Rhodazine DTM Method. The sample volume was between 5 and 10 mL.

Sulphide

For sulphide concentrations lower than 2 mg/L, the Methylene Blue Method was used and for higher concentrations, the Iodometric Method was used.

The Methylene Blue Method gives the total amount of sulphide in a sample, including dissolved H_2S and HS^-, and any acid-soluble metallic sulphides. The coloring reagent reacts with sulphide, resulting in the formation of a blue color and its intensity is measured at a wavelength of 664 nm. An external

calibration curve was used to calculate the concentration of sulphide. The sample volume was reduced from 5 mL in the original method to 1 mL. Standard stock solutions of approximately 100 mg/L sulphide were prepared using boiled and deoxygenated deionized water as described in the method. The stock solution was used to prepare a set of sulphide standards in the range of 0.1-5.0 mg/L for each sulphide sampling event. For each set of standards that were prepared, the concentration of sulphide stock solution was verified using the Iodometric Method of sulphide determination.

The Iodometric method was modified to use a 0.0025 N sodium thiosulphate titrant, 1 mL of standardized iodine solution and 10 mL of sulphide stock solution that had been diluted to approximately 10 mg/L.

Chapter 3
Results

3.1 Organization

The primary purpose of this study was to determine why sulphide appears to inhibit the degradation of *cis*-DCE and VC but has only a minor effect on the degradation rate of TCE. Thus the behavior of sulphide will be presented first, followed by the kinetics and products of degradation of the various chlorinated ethenes. Raman spectroscopy was used to characterize the surface of the granular iron. The effect of sulphide on the corrosion potential of granular iron will also be presented.

3.2 Sulphide

Sulphide profiles for the low sulphide column (5 mg/L, column B) are shown in Figure 4. Over the period of the test, up to 153 PV, there was no apparent migration of the sulphide profiles and sulphide was not detected beyond a distance of 10 cm from the influent end (residence time of 4 hr). According to Hannson et al. (2002) the decline in sulphide concentration is a consequence of precipitation of iron sulphide. Based on the exponential decline in solution concentration with time, iron sulphide solid phases would be present in greatest abundance near the influent end of the column and would not be present in any significant amount beyond a distance of about 10 cm from the influent end.

Sulphide profiles for the column receiving 50 mg/L (Column C) are shown in Figure 5. At early time (54 PV) sulphide concentrations decreased along the column from 50 mg/L to about 10 mg/L. Over time however, the rate of sulphide removal declined such that by 477 PV, only about 20% of the initial sulphide was removed within the column. The results showed that at the high sulphide concentration there was a progressive decline in the amount of sulphide that was being precipitated on the iron surfaces along the column. Furthermore, the fact that there was a decline in concentration across the entire column indicates that iron sulphides would be present across the entire length of the column.

15

Raman spectroscopy was used to characterize the surface of the granular iron at the end of the column experiments. Samples of the iron grains were taken from a port 5 cm from the influent in Column B, with the results shown in Figure 6. The large peak at 670 cm^{-1} represents magnetite (Ritter et al., 2002). FeS peaks are weak (208 cm^{-1} and 280 cm^{-1}) and only 4 spots out of 10 that were examined showed these peaks.

Raman spectroscopy was also used to characterize the iron surface from column C, which received ~50 mg/L sulphide. The iron was taken at the very bottom of the column. Figure 7 shows the Raman Spectroscopy results for this column. There are distinct peaks at 208 cm^{-1} and 280 cm^{-1} showing the presence of FeS on the surface. There is also a peak at 670 cm^{-1} showing magnetite on the surface. All ten spots examined showed the same three peaks, with some variations in peak intensity.

The granular iron from the field site where TCE would degrade but *cis*-DCE and VC would not was also characterized with Raman Spectroscopy. The results are shown in Figure 8. The characteristic peaks for FeS (208 and 280 cm^{-1}) were observed. The magnetite peak at 670 cm^{-1} was also observed. Since the iron from the above ground reactor and also from the high sulphide column showed similar peaks at 208 cm^{-1} and 280 cm^{-1} it can be concluded that iron sulphide was indeed present in the field reactor and at least in this respect, the laboratory tests reproduced the field conditions.

3.3 TCE Degradation

The first set of tests was conducted to examine the behavior of TCE reduction in the presence of sulphide. Six TCE profiles were measured at different PV, for columns A, B and C (Table 1). The profiles for each column were similar in form and showed no consistent trend with the number of PV and thus Figure 9a includes only the mean profile and error bars indicating one standard deviation.

TCE degraded at similar rates in columns A & B, with half-lives of 1.7±0.3 hr and 1.5±0.9 hr. In the high sulphide column (C) TCE degraded somewhat more slowly with a half-life of 5.2±2.2 hr. The half-lives for each sampling event are presented in Table 3. Thus, while the low sulphide concentration did not appear to influence the rate of TCE degradation, the high sulphide concentration resulted in a moderate decline in reaction rate.

The degradation products for TCE were measured in Columns D and E which had influent solutions similar to columns A and B. Figures 10 and 11 show typical degradation profiles for TCE in the control column and in the sulphide column, respectively. In both columns, TCE degraded at approximately the same rate. However, the degradation products differed significantly. In the control column, *cis*-DCE was only detected in very small amounts (<150 µg/L) and no VC or acetylene were detected. Ethene and ethane both appeared at relatively early time in the control column. Ethene reached a maximum of about 20% of the initial TCE at a residence time of 3 hr (~15 cm along the column), then remained relatively constant over the remainder of the column. Ethane, on the other hand, continued to increase, even beyond the time that TCE had disappeared, reaching a maximum in the effluent of almost 80% of the initial TCE. The trend in the carbon mass balance and the ethane profile suggests the presence of an unidentified intermediate that was subsequently transformed to ethane prior to exitin the column.

 In the sulphide column ~10% of the initial TCE appeared as *cis*-DCE, which persisted throughout the column. No VC was detected, but acetylene was detected up to a concentration of 110 µg/L. Ethene began to appear in the column somewhat later than in the control, reached a higher concentration (40% of the initial TCE) at a residence time of about 6 hr and persisted at this concentration for the remainder of the column. Ethane also appeared later than in the control (residence time of 6 hr), and was continuing to increase in concentration at the effluent end. The carbon mass balance at the effluent end was about 82%; however, based on the trend in ethane, there is reason to believe that this would have improved had the residence time been longer. As in the control, the trend in the column mass balance and in ethane suggests the presence of an unidentified intermediate that subsequently degraded to ethane.

After the columns had been run with the individual organics, the source solutions were switched to include TCE (~10 mg/L) and *cis*-DCE (~2 mg/L) (Table 1). Figure 12 shows the degradation of TCE and *cis*-DCE in the control column (A) when they were run separately at the beginning of the experiment compared to the degradation when they were run together at the end of the experiment. TCE degraded more quickly at PV 496 with a half-life of 0.72 hours compared to the TCE at PV 85 which had a half-life of 1.35 hours. c*is*-DCE also degraded in the control column at the end of the experiment with a half-life of 1.96 hours.

Figure 13 shows the degradation of TCE in column C (~50 mg/L sulphide) at the beginning of the experiment (~80 PV) compared to the end of the experiment (485 PV). The half-life for TCE decreased from 7.63 hours at 80 PV to 1.96 hours at 485 PV. It is also clear from Figure 13 that *cis*-DCE was formed from the degradation of TCE and accumulated over the length of the column.

3.4 *cis*-DCE Degradation

The second set of tests was conducted to examine the behaviour of *cis*-DCE in the presence of sulphide. Two profiles of *cis*-DCE concentration were measured at different PV, for each of columns A, B and C. A representative profile for each column is shown in Figure 14.

The kinetics for the degradation of *cis*-DCE was greatly affected by the presence of sulphide in the columns. In both the low sulphide column (B) and the high sulphide column (C) there was little or no degradation of *cis*-DCE for the first 4 hours (10 cm of the column). Beyond this point the *cis*-DCE degraded in the low sulphide column, though at a slower rate than in the control. The Raman Spectroscopy results detected some sulphide precipitate at 5 cm along the column, and based on the dissolved sulphide concentration profiles, sulphide precipitates were expected to be very low beyond about 10 cm along the column. Together, with the *cis*-DCE degradation profiles, the results indicate that the presence of sulphide caused a decline in *cis*-DCE degradation rates. The average half-life was 0.37 hours for the control column (A) and 6.49 hours for the low sulphide column (B). In the high sulphide column (C) there was no measurable degradation of *cis*-DCE.

cis-DCE and its degradation products were measured in columns D and E (Table 1). Figure 15 shows a typical profile for the degradation of *cis*-DCE in the control column (D). *cis*-DCE was transformed to ethene and ethane. Ethene was produced and peaked about half-way through the column and then degraded. Ethane was the major end product with a good carbon mass balance (ranging between 100-125%) along the column.

In the sulphide column, the degradation products from *cis*-DCE were quite different from those in the control column (Figure 16a). *cis*-DCE degraded more slowly and there were much smaller quantities of ethene and ethane produced than in the control column. Ethene was not detected until hour 4 in the sulphide column and its concentration increased thereafter. Ethane was not detected until about half-way through the column. At the end of the column, *cis*-DCE had been transformed to ~25% ethene

18

and 15% ethane. Acetylene was also detected, however it was not detected in the control column (Figure 16b). The mass balance was not complete in the sulphide column, with only 60% of the carbon being accounted for throughout most of the column.

After receiving sulphide at ~7 mg/L for 93 PV the source solutions were switched to *cis*-DCE with no sulphide for column E (Table 1). The column was then run for an additional 45 PV to examine whether *cis*-DCE would degrade once sulphide was removed from the influent. Figure 17 shows *cis*-DCE degradation profiles before and after sulphide removal and compared to the *cis*-DCE profile in the control column. In the control column *cis*-DCE degraded quickly with a half-life of 0.54 hours. When the column was receiving sulphide (PV 125) the half-life was 9.83 hours. However, when the sulphide was removed from the source solution, *cis*-DCE degraded more slowly with a half-life of 13.15 hours. These results indicated that at least on the time scale of these tests, the sulphide precipitates that were deposited on the iron surface will continue to affect the degradation of *cis*-DCE even when sulphide is removed from the influent solution.

3.5 VC Degradation

A third set of tests was conducted to examine the behaviour of VC in the presence of sulphide. Two profiles of VC concentration were measured at different PV, for each of column A, B and C. A representative profile for each column is shown in Figure 18.

Similar to *cis*-DCE, the kinetics for degradation of VC was greatly affected by the addition of sulphide to the columns. In the control column (A) the average half-life was 0.38 hours, compared to the average half-life of 2.75 hours in the low sulphide (B) and 40.41 hours in the high sulphide column (C). VC in the low sulphide column (B) did not start to degrade until after 3 hour of residence time (10 cm along the column).

The degradation products for VC were measured in columns D and E (Table 1). Figure 19 shows a typical degradation profile for VC in the control column at PV 95. VC degraded quickly and both ethene and ethane were produced. At the end of the column all of the VC had been transformed to ethane. There was a good carbon mass balance along the entire length of the column.

The degradation products of VC were quite different in the sulphide column. Figure 20 shows a degradation profile for VC in column E at PV 87. VC did not degrade until half-way through the column. At ~15 cm (3.5 hour residence time) into the column small amounts of ethene and ethane were detected. At the end of the column 35% of the VC had been transformed to ethene and 18% to ethane.

3.6 1,1-DCE Degradation

A fourth set of tests was conducted to examine the behaviour of 1,1-DCE in the presence of sulphide. Two profiles of 1,1-DCE concentration were measured at different PV, for each of columns A and C. A representative profile for each column is shown in Figure 21a.

In the control column 1,1-DCE degraded quickly and was below the detection limit by the third hour. However, in the sulphide column very little 1,1-DCE degraded. At the end of the column there was still ~80% of the initial 1,1-DCE present. The average half-life in the control column was 0.34 hours compared to 23.9 hours for the sulphide column (Table 3). VC was only detected in the sulphide column (Figure 21b), though at very low concentrations.

3.7 *trans*-DCE Degradation

The effect of sulphide on the degradation of *trans*-DCE was also tested with columns A and C. Two profiles of *trans*-DCE were measured at different PV. A representative profile for each column is shown in Figure 22a. The average half-life in the sulphide column was 5.34 hrs compared to only 0.27 hr in the control (Table 3). Similar to 1,1-DCE, VC was only detected in the sulphide column (Figure 22b), reaching a maximum of about 2% of the influent *trans*-DCE.

3.8 Corrosion Potential

The corrosion potential was measured with and without the presence of sulphide in columns D and E during the addition of TCE, *cis*-DCE and VC (Table 1). The data was collected after the initial auto-reduction process was completed (11 days). The average value for the corrosion potential was then calculated and converted to SHE. pH was also measured. The variation in pH of the two columns was taken into consideration using the Nernst equation, which states that an increase in one pH unit results in a decrease in potential of 59 mV at 25°C under standard conditions.

E=E°-0.0591pH

Figure 23 shows the corrosion potential for TCE over 7 days. Due to the low concentration of sulphide in the source solution the only port that was receiving sulphide was the bottom port of column E. For the ports without sulphide the average corrosion potential was -608 mV compared to the sulphide at -536 mV. Therefore the sulphide caused an average shift of 72 mV.

The corrosion potential measurements when columns D and E were receiving *cis*-DCE are shown in Figure 24. The measurements were taken for 10 days. Again only the bottom port of column E was receiving sulphide. The average value for the ports without sulphide was -592 mV compared to the port that was receiving sulphide where the average was -538 mV. Therefore the sulphide caused an average positive shift of 57 mV when the column was receiving *cis*-DCE and sulphide.

The corrosion potential measurements when columns D and E were receiving VC are shown in Figure 25. Measurements were taken over 8 days. The bottom port of column E was the only port receiving sulphide. The average value for the ports with sulphide was -540 mV compared to the port that was not receiving sulphide where the average was -628 mV. Therefore the sulphide caused an average shift of 88 mV when the column was receiving VC and sulphide. A comparison of the average corrosion potentials is shown in Table 5.

3.9 Electrochemical Experiments

Differential pulse voltammetry on a Hg drop electrode was used to determine the reduction potential of TCE to *cis*-DCE and *cis*-DCE to VC. The differential pulse voltammograms for TCE and *cis*-DCE are presented in Figure 26.

The measured reduction potential for TCE to *cis*-DCE was -0.727 V. To ensure the reduction process was being completed, the products from the degradation of TCE were measured and confirmed that *cis*-DCE, *trans*-DCE and 1,1-DCE were being produced from the reduction of TCE. The results indicated that the majority of the TCE was transformed to *cis*-DCE with trace amounts of 1,1-DCE and *trans*-DCE at the end of the experiment. The measured reduction potential for *cis*-DCE to VC was -0.803 V. When *cis*-DCE was injected, VC was produced.

Chapter 4

Discussion

4.1 Summary of Key Observations:

- Sulphide quickly precipitates on the iron surface. In the low sulphide column (B) the sulphide was no longer detectable in the solution phase after 15 cm (3.5 hr residence time) into the column. In the high sulphide column (C) dissolved sulphide concentrations decreased across the entire column, suggesting that sulphide precipitates formed throughout the column.

- Raman Spectroscopy results confirmed the presence of sulphide on the surface of the granular iron, abundant in the high sulphide column and lesser amounts in the low sulphide column.

- Low sulphide concentrations did not appear to influence the rate of TCE degradation, however at the higher sulphide concentrations there was a moderate decline in reaction rates.

- *cis*-DCE, 1,1-DCE and VC did not degrade by more than 20% over the length of the column when sulphide was present at higher concentrations. Though inhibited near the influent end of the column, degradation appeared to proceed once the sulphide concentrations in solution were below the detection limit in the low sulphide column.

- The degradation products for TCE, *cis*-DCE and VC were affected by the presence of sulphide. *cis*-DCE began to accumulate from the degradation of TCE in the sulphide column and acetylene was only detected when sulphide was present. The production of ethane was reduced when sulphide was present in the column whereas there was complete conversion in the control columns.

- *trans*-DCE degraded, though more slowly in the presence of sulphide. Approximately 60% of the influent concentration was degraded over the length of the high sulphide column.

- The iron corrosion potential shifted in a positive direction an average of 71 ± 13 mV when sulphide was present for TCE, *cis*-DCE and VC.

- The reduction potential for TCE to *cis*-DCE was measured at -727 mV and for *cis*-DCE to VC was -803 mV.

- Trends in the carbon mass balance and in the ethane profiles suggested the presence of an unidentified intermediate. This was particularly evident in the columns receiving sulphide.

Clearly the most striking feature of the data is the preferential passivation of the iron, apparently caused by the presence of sulphide, towards the DCE isomers and VC, relative to the minor effect with respect to TCE. Three possible explanations for this behavior are proposed:

1. When sulphide is present there is a significantly different shift in corrosion potential in the presence of *cis*-DCE or VC compared to TCE, which allows TCE to degrade but not *cis*-DCE or VC.
2. The presence of sulphide causes a shift in the corrosion potential such that the corrosion potential is sufficiently low for TCE to continue to degrade but is too high for the DCE isomers and VC to degrade.
3. Sulphide, by some means, blocks certain degradation pathways but not others.

Considering the first hypothesis, the corrosion potential shifts in the presence of sulphide and TCE, *cis*-DCE or VC are the same (+75 mV) for all three compounds,therefore a differential shift in corrosion potential can not be the cause of the preferential passivation and thus the first hypothesis does not apply.

The second hypothesis depends upon the relative reduction potentials of TCE, *cis*-DCE and VC and the processes responsible for the degradation of these compounds. The reduction of chlorinated ethenes by iron may proceed through one- or two-electron transfer processes. The DPV measurements showed that the one-electron transfer potential for TCE to *cis*-DCE was -727 mV and for *cis*-DCE to VC was -803 mV. The measured value is quite similar to the calculated reduction potential for *cis*-DCE to VC of -890 mV reported by Roberts et al. (1996), providing a degree of confidence in the measured values. The lowest corrosion potential measured in this study using Connelly iron was between -650 mV and -675 mV and thus the one-electron transfer process for either TCE or *cis*-DCE would not be thermodynamically possible. Also, sulphide causes a positive shift in potential so when sulphide is present, one electron transfer would be even more unlikely.

Two-electron transfer processes include reductive β-elimination and hydrogenolysis. Using electrolytic Fisher iron (99.99% pure) in batch experiments, Arnold and Roberts (2000) showed that for TCE degradation, reductive β-elimination was the major degradation pathway (97%) and hydrogenolysis was a minor contributor (3%). TCE can not be transformed to *cis*-DCE by β-elimination and thus, following Arnold and Roberts (2000), the *cis*-DCE that accumulated in the sulphide columns during the degradation of TCE, presumably followed the hydrogenolysis pathway.

This being the case, it appears that the hydrogenolysis pathway was not significantly affected by the presence of sulphide.

It was calculated in Roberts et al. (1996) that the potential for reductive β-elimination of TCE is -599 mV. This value was slightly less negative than the measured corrosion potential in the control columns, suggesting that reductive β-elimination can proceed in the absence of sulphide. However, when sulphide was present the ranges of the corrosion potentials shifted from between -675 and -600 mV to between -550 and -525 mV for TCE, *cis*-DCE and VC. This shift in corrosion potential could be caused by the formation of FeS films as seen in experiments with very pure iron (Hansson, 2007). The shift in corrosion potential makes the corrosion potential less than the required -599 mV, making the β-elimination pathway thermodynamically unfavorable. However, there could be localized areas on the iron which have a lower corrosion potential due to cracks or edges which allows the β-elimination pathway to proceed. Also the potentials measured in the columns are an average of the local iron close to the tip of the electrodes, therefore other areas may have different values of corrosion potential. Thus the difference between the measured potential in the presence of sulphide (~-540mV) and the required potential for β-elimination (-599 mV) may not be significant, since TCE continued to degrade in the presence of sulphide, it is clear that sulphide does not inhibit β-elimination, the main pathways for the degradation of TCE.

It was observed in this study that *cis*-DCE did not degrade by more than 20% over the length of the column when sulphide was present. *cis*-DCE should degrade by reductive β-elimination at -568 mV or by hydrogenolysis at a potential of -407 mV (Roberts et al., 1996). When sulphide was present the iron corrosion potential did not exceed -540 mV, and thus hydrogenolysis should still proceed. However, the measured potentials and the required potentials for reductive β-elimination are quite close a definite conclusion can not be made. Therefore, the corrosion potential in the columns should be low enough for hydrogenolyis and possibly reductive β-elimination to occur even when sulphide is present. However, since *cis*-DCE did not degrade when sulphide was present the results suggest that *cis*-DCE does not degrade by either hydrogenolysis or reductive β-elimination.

There is considerably more evidence in support of the third hypothesis, that sulphide blocks certain degradation pathways but not others, resulting in TCE being able to degrade whereas the DCE isomers and VC do not. A striking difference between the sulphide and control columns was that

acetylene was only detected in the columns receiving sulphide and that much less ethane appeared in the sulphide columns compared to the control columns. Table 6 compares the amounts of ethene and ethane in the control and sulphide columns at about 3.5 hr of residence time. Arnold and Roberts (2000) suggested that hydrogenation was responsible for the transformation of acetylene to ethene and ethene to ethane. Since acetylene was observed in the columns receiving sulphide, and there was much less ethane produced in the sulphide columns, it is suggested that the pathways between acetylene and ethene and also the pathway between ethene and ethane, hydrogenation, is inhibited by the presence of sulphide. Furthermore, though the hydrogenation process was not specified in Arnold and Roberts (2000), hydrogenation usually involves a catalyst (Raymond, 2006). It was proposed in Li and Farrell (2000) that TCE could degrade by catalytic hydrogenation. Odziemkowski et al. (2000) also suggested that catalytic hydrogenation was the process that degraded N-nitrosodimethylamine (NDMA) by granular iron. Even though iron is not known as a catalyst, the impurities found on the surface of commercial iron could provide the needed catalyst for this reaction (Matheson and Tratnyek, 1994). It is also well known that catalysts are deactivated by reduced sulphur compounds (Li and Farrell, 2000). The literature provides evidence that certain reactions with granular iron are enhanced by catalysis and the results of this study, the accumulation of acetylene and ethene, indicates that sulphide an be a catalysis inhibitor in iron degradation systems. These observations provide a rational explanation for the apparent preferential passivation of iron towards *cis*-DCE and VC relative to TCE. In brief, it is proposed that the catalytic hydrogenation pathways shown in Figure 1 are inhibited by the presence of FeS on the iron surface.

Based on product distributions, it is well established that TCE degrades by reductive β-elimination (Arnold and Roberts, 2000 and Li and Farrell, 2000). This reaction is not known to be enhanced by catalysis; and based on the results of this study, the β-elimination reaction is not influenced by the presence of FeS, resulting in the continuing high rates of TCE degradation in the presence of sulphide. With or without sulphide, most of the TCE would be transformed to chloroacetylene, which is highly unstable, and based on Figure 1, would be rapidly transformed to acetylene and acetylene is subsequently transformed to ethene by catalytic hydrogenation. The fact that acetylene was detected in the columns where sulphide was present, but not in the controls, suggests that the catalytic transformation was inhibited by sulphide. Though relatively small amounts of acetylene were detected, this could well be an analytical problem as suggested by the trends in carbon mass balance. That is, in the control columns there was a good mass balance over the entire column, while in the

25

presence of sulphide, a significant amount of carbon appeared to be missing in the region of the column where TCE was degrading most rapidly. The missing carbon is believed to be acetylene that was not accounted for in the analytical procedure. The fact that most of the carbon was ultimately accounted for suggests that the catalytic hydrogenation of acetylene to ethene was inhibited but not blocked once the sulphide was out of the system.

Further, following Figure 1, a small proportion of TCE degrades to the DCE isomers (primarily *cis*-DCE) by hydrogenolysis. The fact that TCE degradation in the presence of sulphide results in an accumulation of *cis*-DCE (Figure 13 for example) suggests that sulphide does not inhibit hydrogenolysis and that the reaction process for TCE to *cis*-DCE is indeed hydrogenolysis.

Though Arnold and Roberts (2000) proposed the transformation of *cis*-DCE to VC to be a hydrogenolysis reaction, their experimental results would be equally consistent with catalytic hydrogenation. Indeed, this was proposed by Li and Farrell (2000). Consistent with the results of the present study, it is proposed that catalytic hydrogenation is the primary transformation process for *cis*-DCE, and that sulphide acts as a catalyst poison, significantly inhibiting this process, leading to substantially reduced degradation rates in the presence of sulphide. Though Arnold and Roberts (2000) suggested β-elimination with acetylene as the primary product for *cis*-DCE degradation, this is not consistent with the present results. In the absence of sulphide, no acetylene was detected and in the presence of sulphide only trace amounts were detected. It is therefore proposed that β-elimination is a minor pathway for *cis*-DCE degradation and, as in the case of TCE, this pathway is not inhibited by sulphide.

As shown in Figure 1, the primary degradation pathways for 1,1-DCE and VC are similar to those for *cis*-DCE, though VC does not include a β-elimination pathway. The experimental results for these compounds were almost identical to those obtained for *cis*-DCE, indicating greatly reduced rates of degradation in the presence of sulphide. Thus a similar explanation would appear to apply. That is, the primary pathway is believed to be catalytic hydrogenation, and this pathway is significantly impeded through catalyst poisoning by sulphide. Figure 1 suggests α-elimination as a possible pathway for 1,1-DCE. This pathway would not be poisoned by sulphide and thus our results suggest that this is not a significant pathway.

26

The results for *trans*-DCE differed from those of *cis*-DCE and 1,1-DCE in that *trans*-DCE continued to degrade in the presence of sulphide, but at a significantly lower rate than in the control column. In Figure 1, *trans*-DCE is shown to degrade by both hydrogenolysis and β-elimination (as in the case of *cis*-DCE). As for *cis*-DCE, is it proposed that hydrogenolysis be replaced by catalytic hydrogenation and that this pathway is inhibited as a result of catalytic poisoning by sulphide. Unlike *cis*-DCE however, it appears that the β-elimination pathways is significant, and because β-elimination is not inhibited by sulphide, significant degradation of *trans*-DCE continues in the presence of sulphide.

Figure 27 is a revised chart of degradation pathways for TCE. It is similar to Figure 1, expect that in most cases the hydrogenolysis pathways have been removed. The exceptions are the transformation of TCE to the DCE isomers, though these are generally minor pathways in any case. The hydrogenolysis pathway for the conversion of chloroacetylene to acetylene also remains, though because of the high instability of chloroaceylene the nature of the pathway is uncertain. The α-elimination pathway for 1,1-DCE is also not shown in Figure 27.

While the results of this study are of practical important in the design of PRBs in sitewaters where sulphate and sulphide are present in groundwater, the results also provide new insights concerning the degradation pathways for chlorinated ethenes, the most common halogenated organic contaminants in groundwater.

Chapter 5
Conclusion

The conclusions for this study are:

1. TCE mainly degrades by reductive β elimination which is not interfered with by the presence of sulphide.

2. It appears that *cis*-DCE, 1,1-DCE and VC degrade by catalytic hydrogenation which could be poisoned by the presence of sulphide, causing severely reduced degradation rates.

3. It is proposed that *trans*-DCE can degrade by either reductive β elimination or catalytic hydrogenation. It seems that the sulphide does not interfere with reductive β elimination therefore it can still proceed even when sulphide is present. However, catalytic hydrogenation may be poisoned by sulphide which causes the degradation rates for *trans*-DCE to be lowered when sulphide is present.

4. TCE and *cis*-DCE should not be able to degrade by one-electron transfer with Connelly iron since the corrosion potential of the iron does not reach a low enough potential for this process to proceed.

The results presented in this work have major implications for granular iron PRB design when sulphate or sulphide is present. If groundwater contaminated by TCE also contains sulphide, the particular care must be taken in PRB design. Site water should first be tested in a laboratory setting to determine if the sulphide concentrations are high enough to cause an accumulation of *cis*-DCE and VC. The PRB may have to be designed in such a way that the sulphide precipitates out first and then TCE and its intermediate products can degrade to ethane. Since sulphide is usually formed from sulphate, more research is needed to determine the specific effects of sulphate on the degradation of TCE. Treatment of the sulphate before it is transformed to sulphide may also improve the performance of the granular iron PRB.

Table 1: Operational History of Columns

Column	Porosity (n)	Pore volume (mL)	History of Influent Solution	Residence Time (hr)	CPM*
A – Control	0.55	80.1	Milli-Q Water → TCE →*cis*-DCE → VC → *trans*-DCE → 1,1 DCE→ TCE with *cis*-DCE	6.4-7.9	No
B – Low Sulphide (5 mg/L)	0.55	81.4	Milli-Q Water → TCE → *cis*-DCE → VC	6.7-7.3	No
C – High Sulphide (50 mg/L)	0.54	80.0	Milli-Q Water → TCE →*cis*-DCE → VC → *trans*-DCE → 1,1 DCE → TCE with *cis*-DCE	6.3-8.5	No
D – Control	0.51	115.3	Milli-Q Water →TCE → *cis*-DCE → VC→ *cis*-DCE	8.8 – 9.4	Yes
E –Sulphide (7 mg/L)	0.53	123.4	Milli-Q Water →TCE → *cis*-DCE→ VC→ *cis*-DCE with no sulphide	9.6-10.1	Yes

Table 2: Method Detection Limits for compounds

Compound	MDL (µg/L)
Trichloroethene (TCE)	1.0
Vinyl Chloride (VC)	1.3
trans-1,2-Dichloroethene (*trans*-DCE)	2.4
cis-1,2-Dichloroethene (*cis*-DCE)	1.3
Methane	0.5
Ethene	0.5
Ethane	0.4
Acetylene	3
Sulphide	1.0 mg/L

Table 3: Half-lives in Hours for Columns A, B and C

TCE					
Column A (Control)		*Column B (Low Sulphide)*		*Column C (High Sulphide)*	
PV 20	1.74	PV 29	0.86	PV 19	2.38
PV 33	2.11	PV 45	1.43	PV 31	5.14
PV 43	1.78	PV 94	2.77	PV 47	3.15
PV 59	1.85	PV 121	2.44	PV 55	5.13
PV 75	1.55	PV 141	0.94	PV 68	7.07
PV 85	1.35	PV 166	0.82	PV 80	7.63
PV 496	0.72			PV 485	1.95
cis-DCE					
Column A (Control)		*Column B (Low Sulphide)*		*Column C (High Sulphide)*	
PV 180	0.38	PV 264	5.86	PV 176	33.01
PV 190	0.37	PV 292	7.12	PV 185	70.73

VC					
Column A (Control)		*Column B (Low Sulphide)*		*Column C (High Sulphide)*	
PV 263	0.37	PV 255	2.59	PV 314	36.67
PV 274	0.39	PV 259	2.89	PV 347	44.15

1,1-DCE			
Column A (Control)		*Column C(High Sulphide)*	
PV 412	0.31	PV 390	26.46
PV 442	0.48	PV 428	21.22

trans-DCE			
Column A (Control)		*Column C (High Sulphide)*	
PV 290	0.31	PV 275	4.50
PV 310	0.23	PV 296	6.12
PV 341	0.22	PV 331	3.32
PV 365	0.29	PV 356	4.00

Table 4: End products for the degradation of TCE, *cis*-DCE and VC

Parent Compound	Products	Average mass recovery at end of column D as % (control)	Average mass recovery at end of column E as % (sulphide)
TCE	TCE	0.70	0.16
	cis-DCE	0.20	8.44
	trans-DCE	0.01	0.13
	1,1-DCE	0.00	0.12
	VC	0.00	0.00
	Acetylene	0.00	0.00*
	Ethene	18.51	31.24
	Ethane	72.87	51.26
	5.1.1 Total	**92.30**	**91.34**
***cis*-DCE**	*cis*-DCE	0.83	21.55
	VC	0.35	0.08
	Acetylene	0.00	0.12
	Ethene	6.66	25.89
	Ethane	111.68	15.32
	Total	**119.53**	**62.96**
VC	VC	0.00	62.62
	Ethene	0.00	35.24
	Ethane	103.02	17.64
	Total	**103.02**	**115.51**

Table 5: Average Corrosion Potential Measurements

	Average Corrosion Potential Measurement (mV)		
	Column E low port (with sulphide)	Average CPM for ports in control column	Changed
TCE	-536	-608	72
cis-DCE	-538	-592	54
VC	-540	-628	88

Table 6: Production of Ethene and Ethane in 20 cm columns at the 3.5 hour residence point (Results are shown in % of original C)

	TCE control	TCE sulphide	*cis*-DCE control	*cis*-DCE sulphide	VC control	VC sulphide
Ethene %	25	17	37	5	32	5
Ethane%	22	4	35	Non detect	68	2
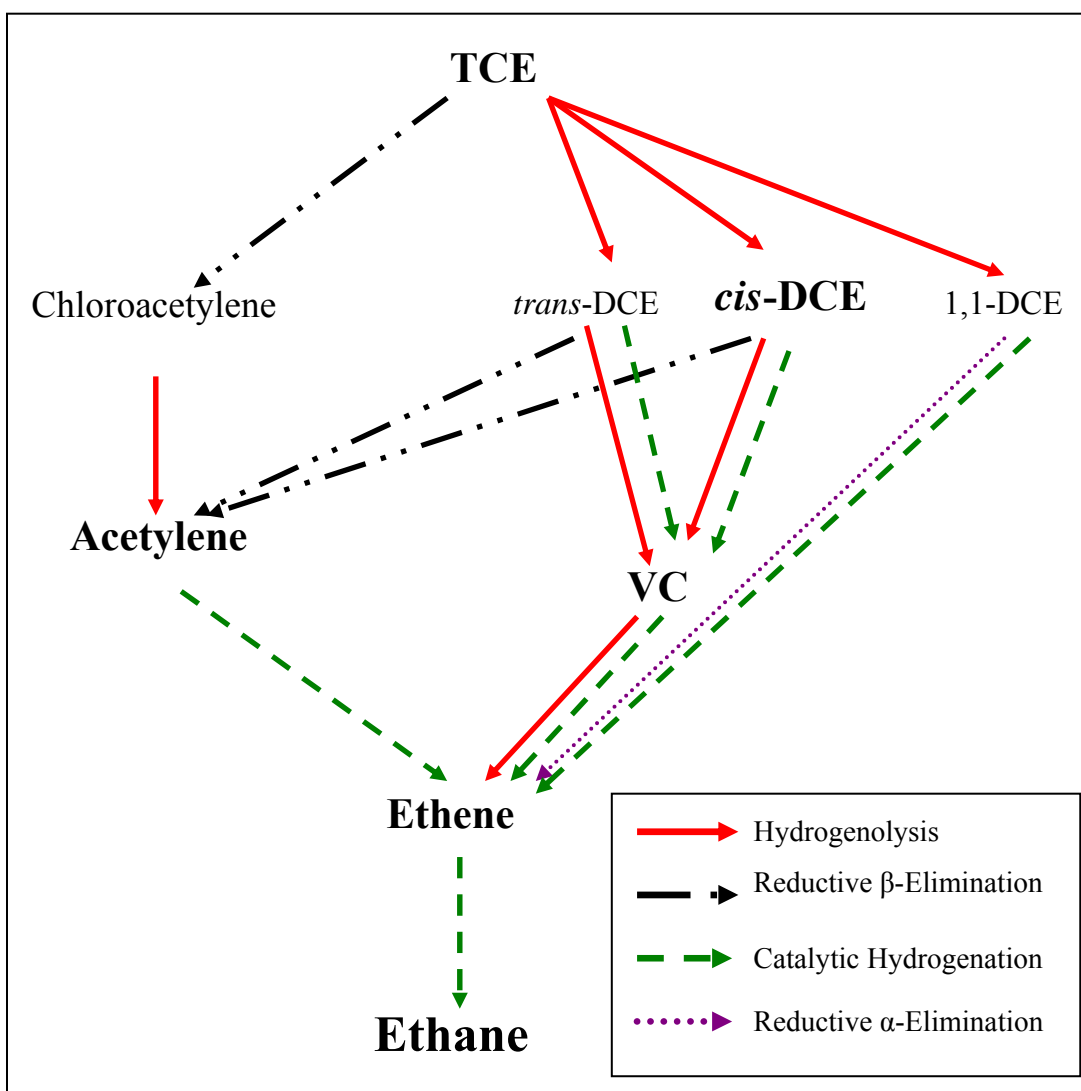
Figure 1: The proposed pathways for the degradation of TCE (adapted from Arnold and Roberts, 2000 and Li and Farrell, 2000).
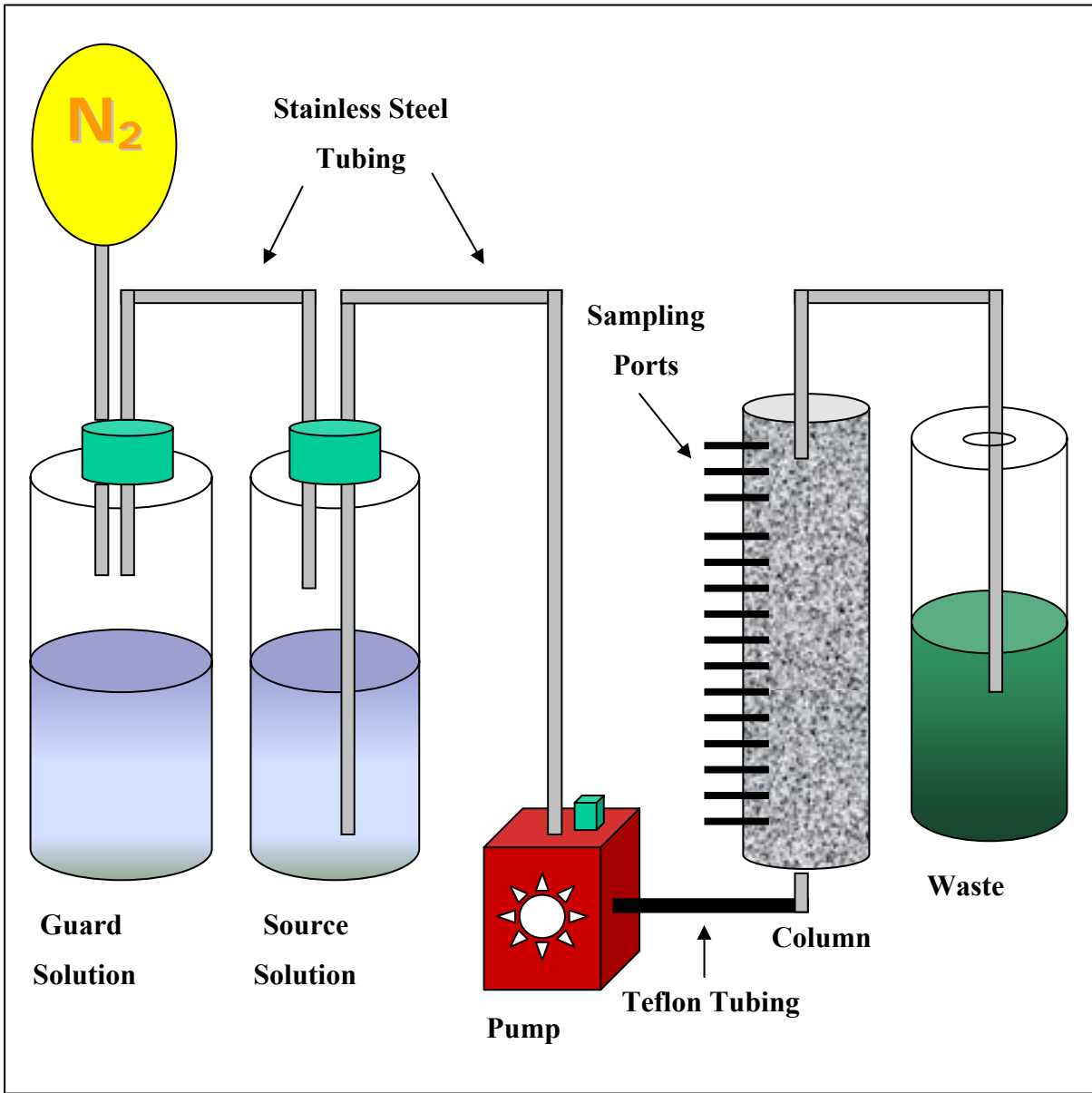
Figure 2: General set-up for columns
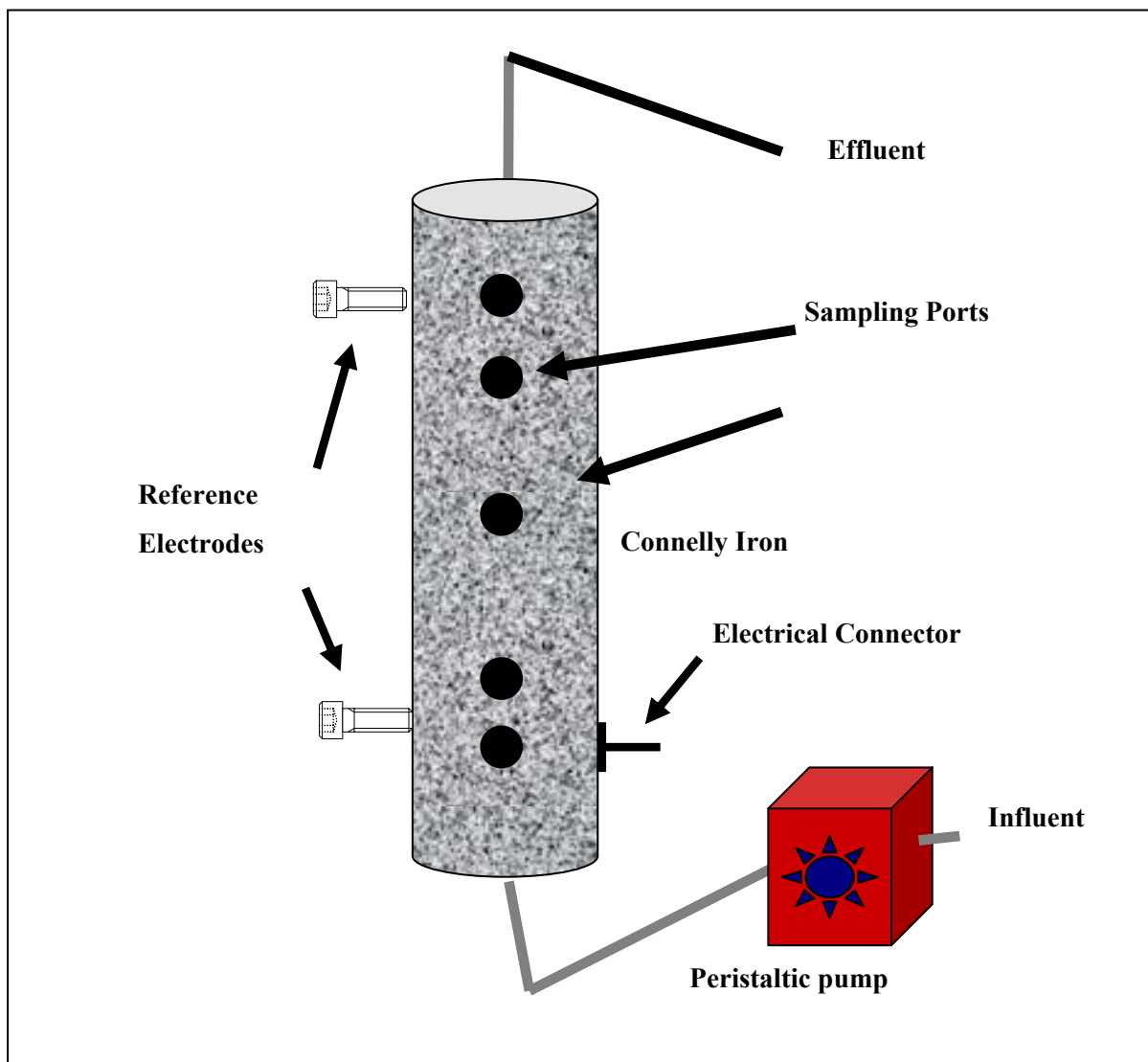
Figure 3: Set-up for columns D and E with corrosion potential measurements
(adapted from Lu, 2005).
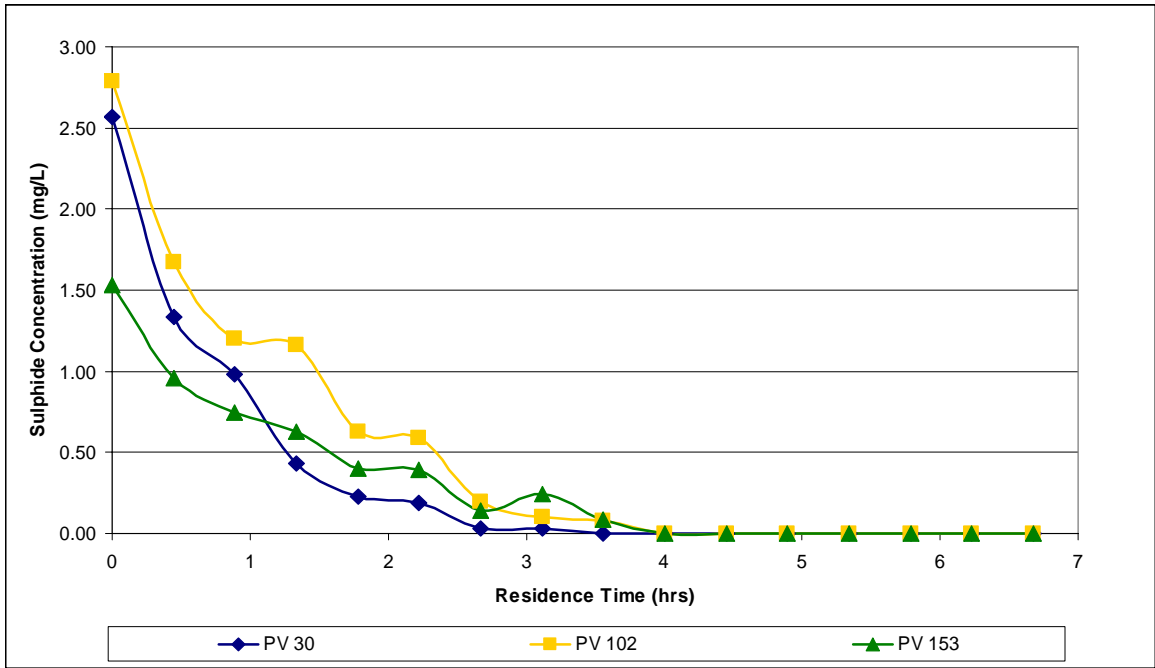
Figure 4: Sulphide profiles for the column receiving the lowest concentration of sulphide (Column B).
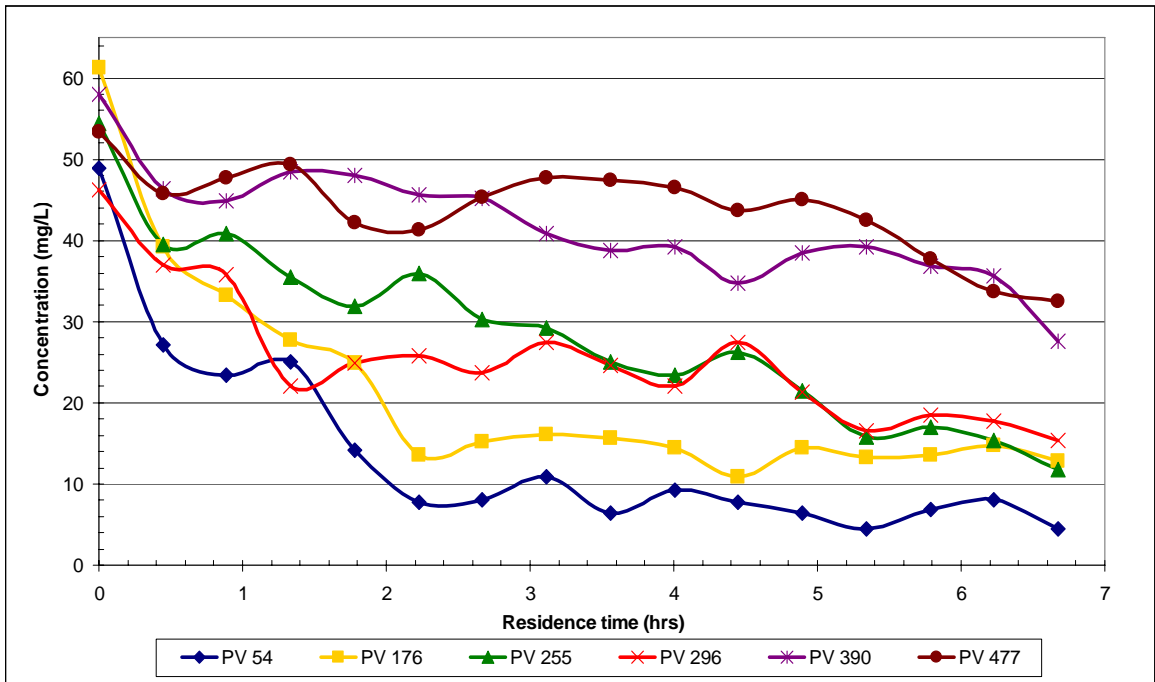
Figure 5: Sulphide profiles for the column receiving the highest concentration of sulphide (Column C).
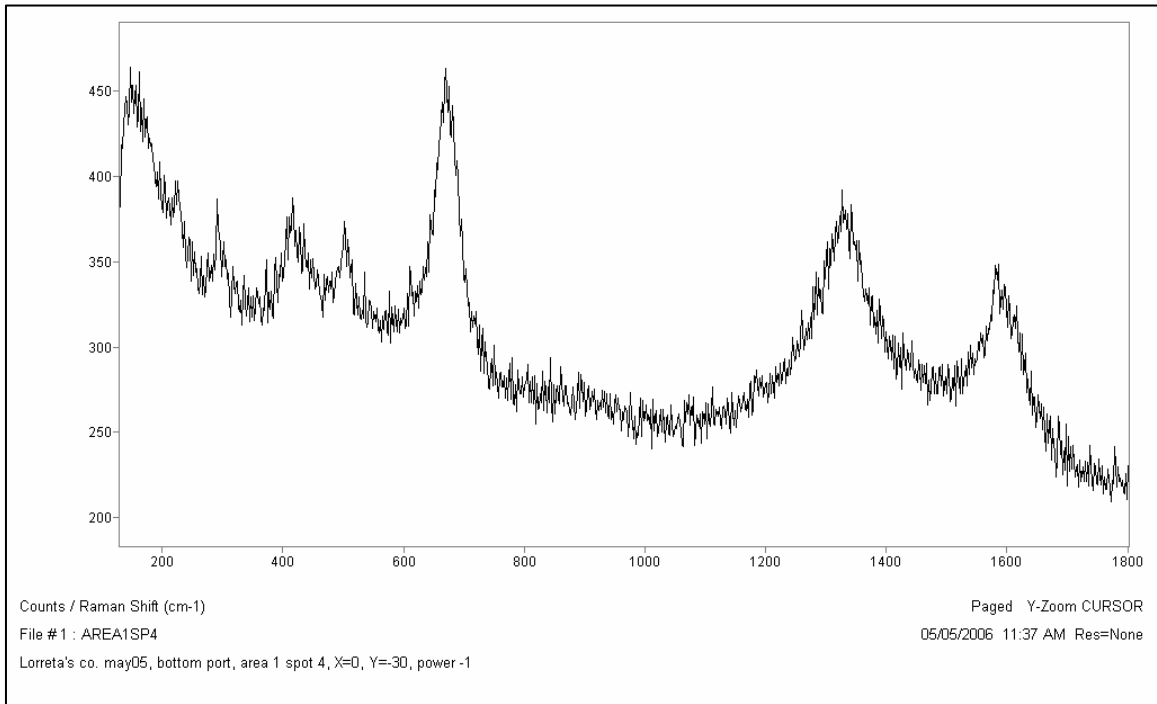
Figure 6: Raman spectroscopy results from iron for Column B (~5 mg/L) 5 cm from the influent end.
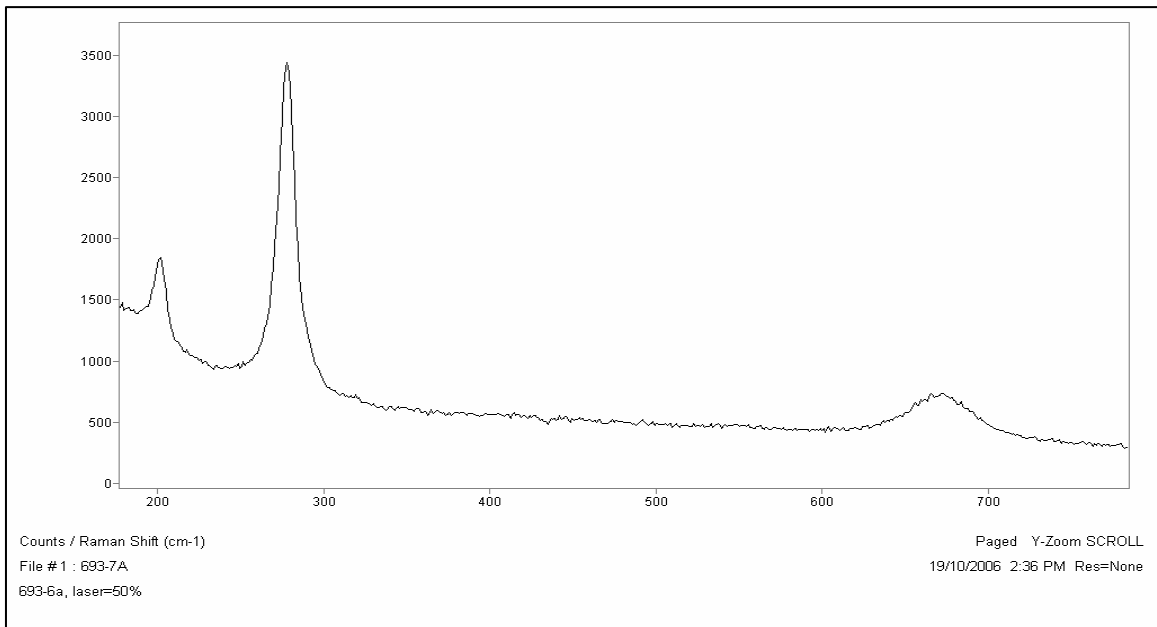
Figure 7: Raman spectroscopy results from Iron from High Sulphide Column (C). The peaks at 208 cm-1 and at 280 cm-1 indicate the presence of FeS on the iron surface.
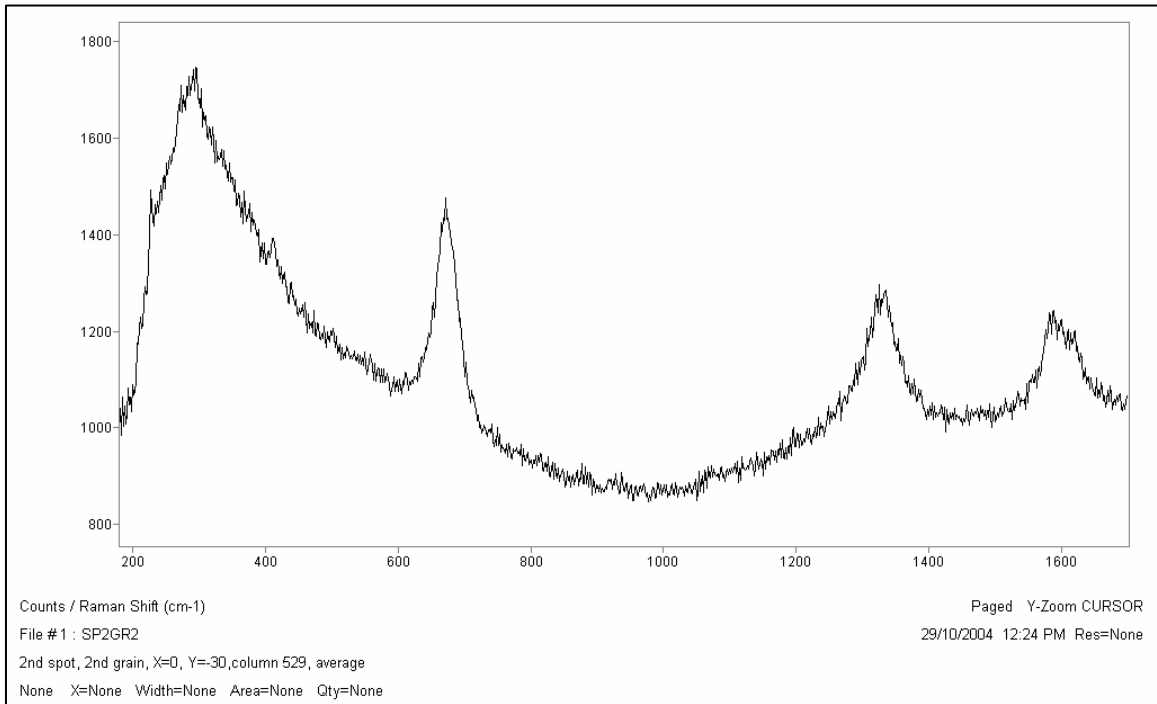
Figure 8: Raman spectroscopy results from iron cored from above field reactor. The peaks at 208 cm-1 and at 280 cm-1 indicate the presence of FeS on the iron surface.
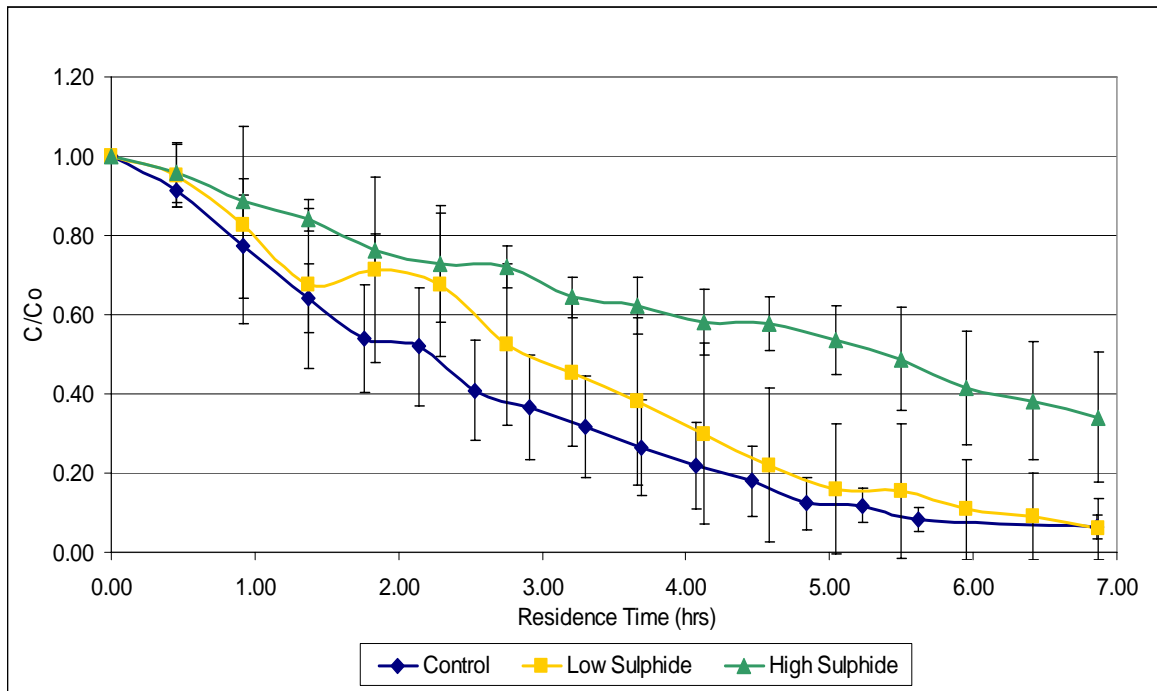
Figure 9: Average degradation profile for TCE in Columns A (Control), B (Low Sulphide) and C (High Sulphide).
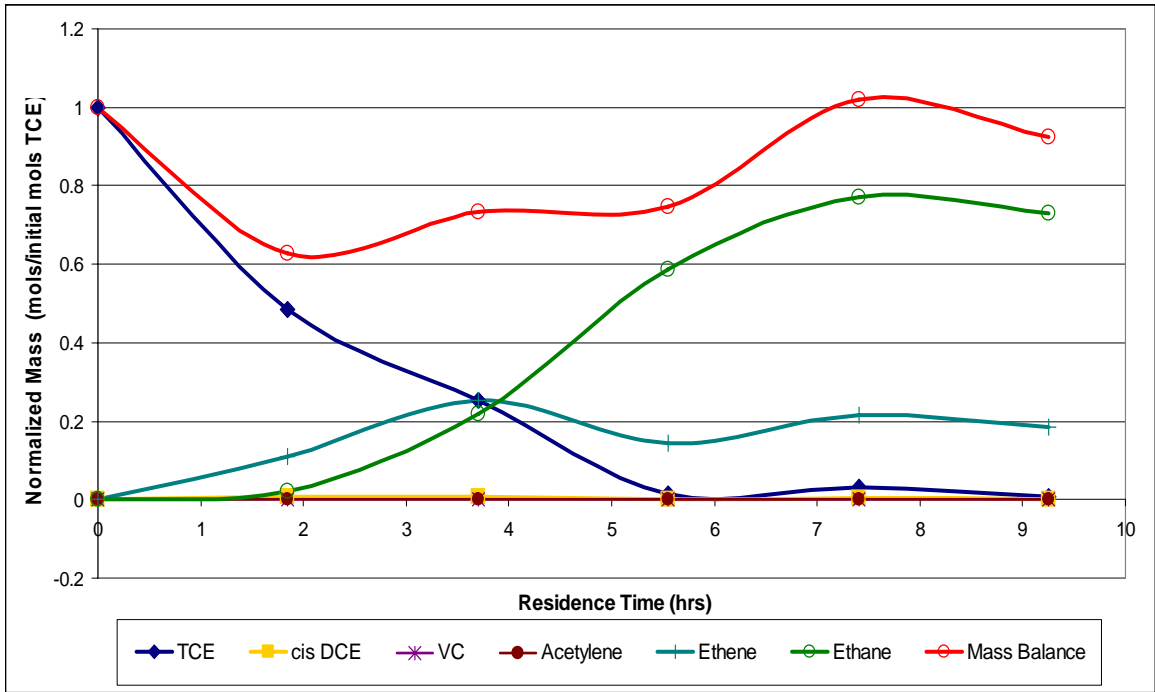
Figure 10: Degradation profile for TCE in the control column (D) with an influent of 9.9 mg/L TCE at PV 95.
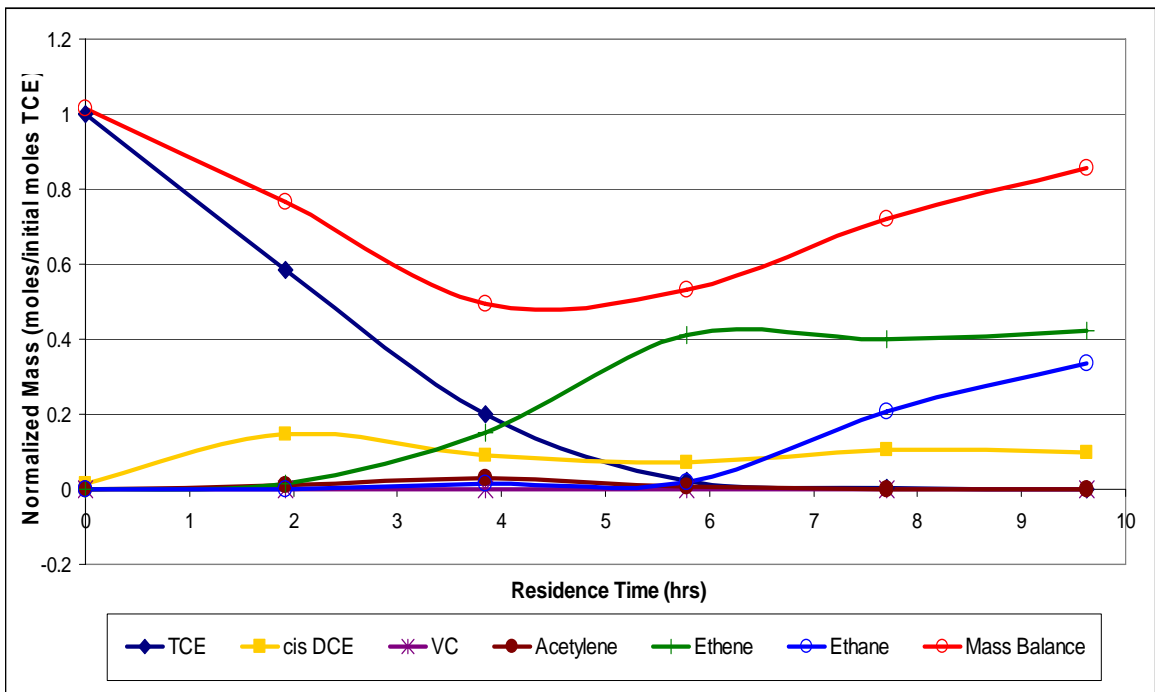
Figure 11: Degradation profile for TCE in column E with an influent of 9.1 mg/L TCE and ~7 mg/L sulphide at PV 72.
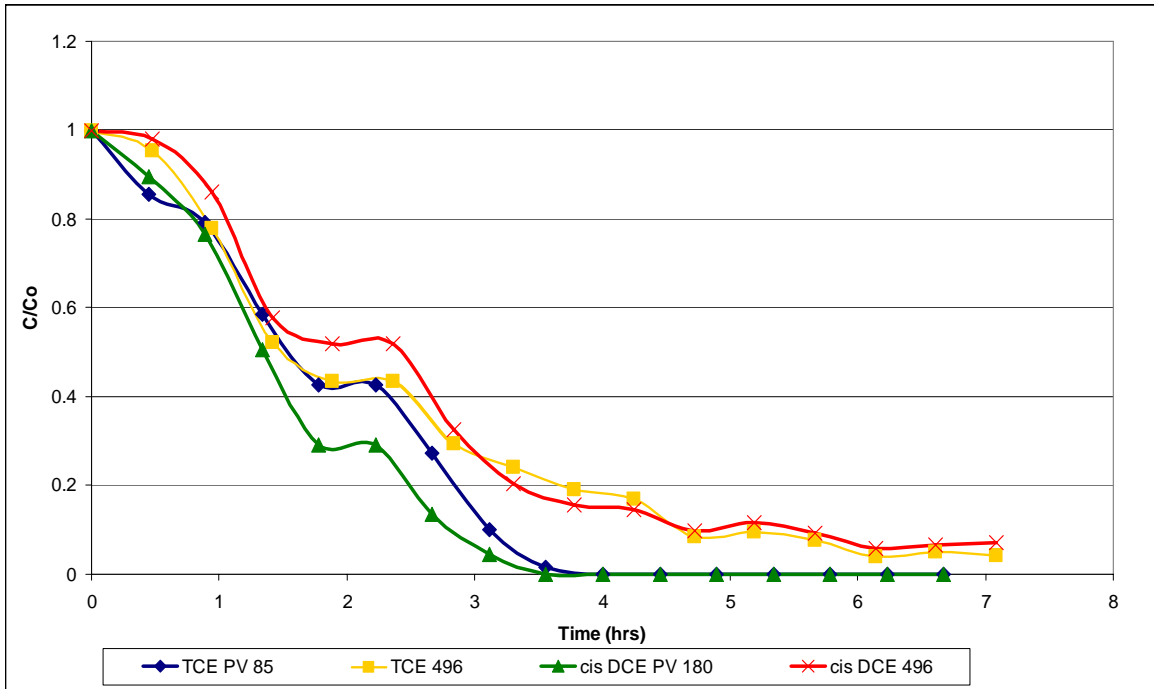
Figure 12: Comparison of the degradation of TCE and *cis*-DCE in column A (Control) at the beginning and at the end of the experiment.
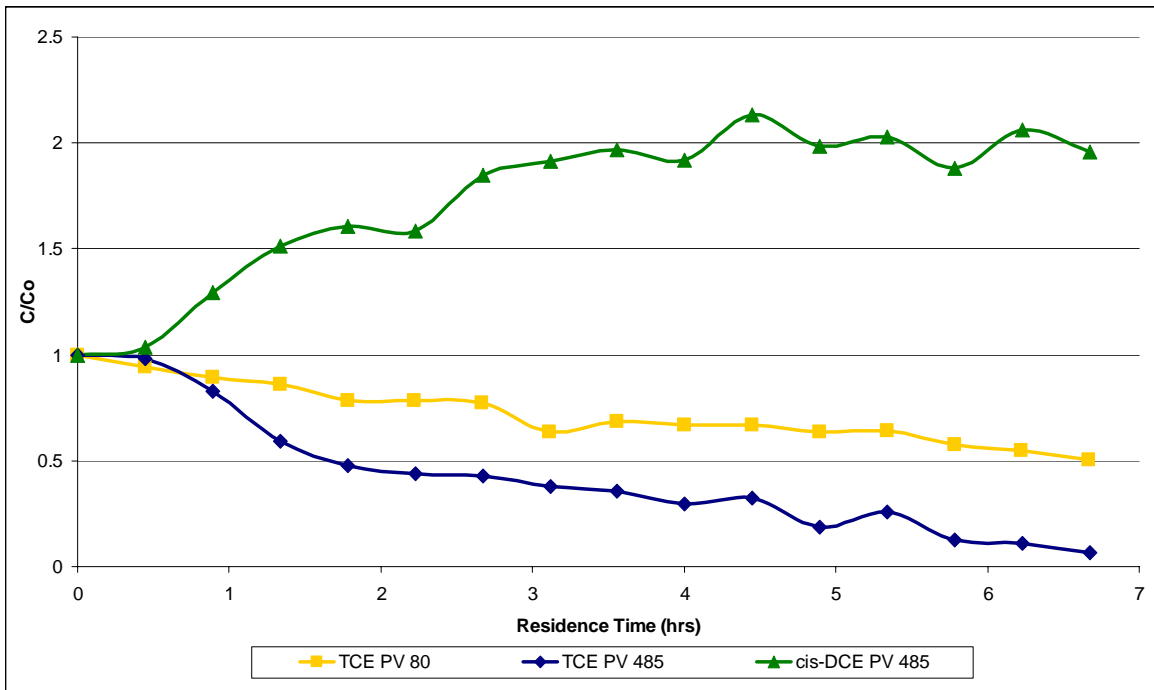
Figure 13: Comparison of the degradation of TCE and *cis*-DCE in Column C (~50 mg/L) sulphide at the beginning and at the end of the experiment.
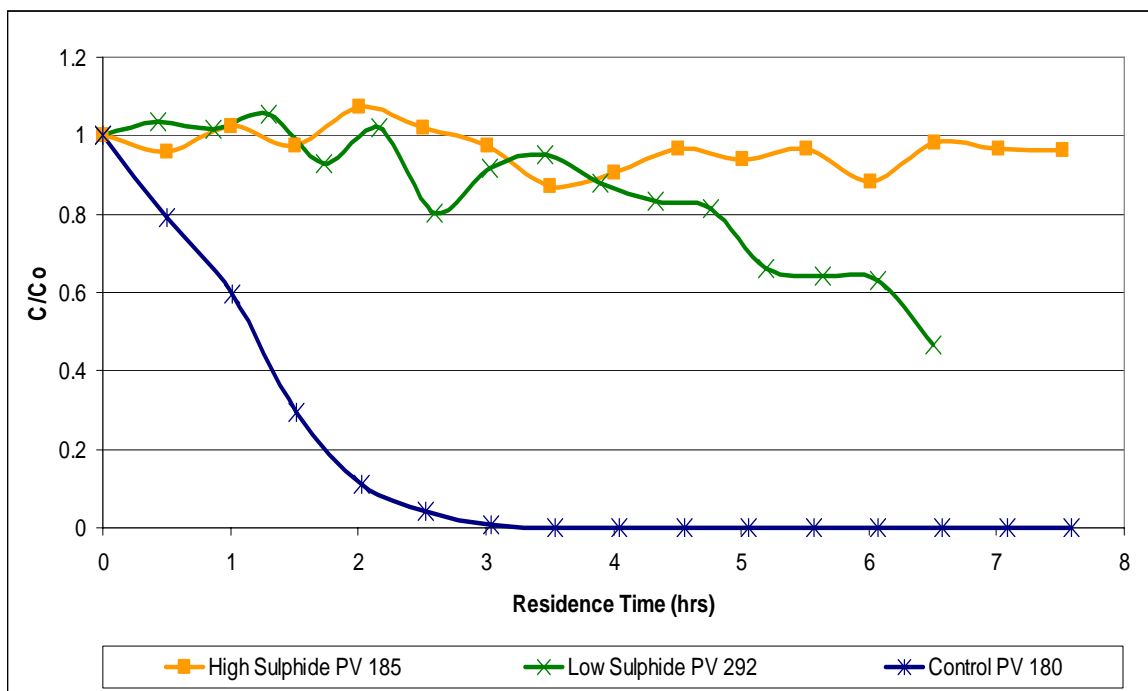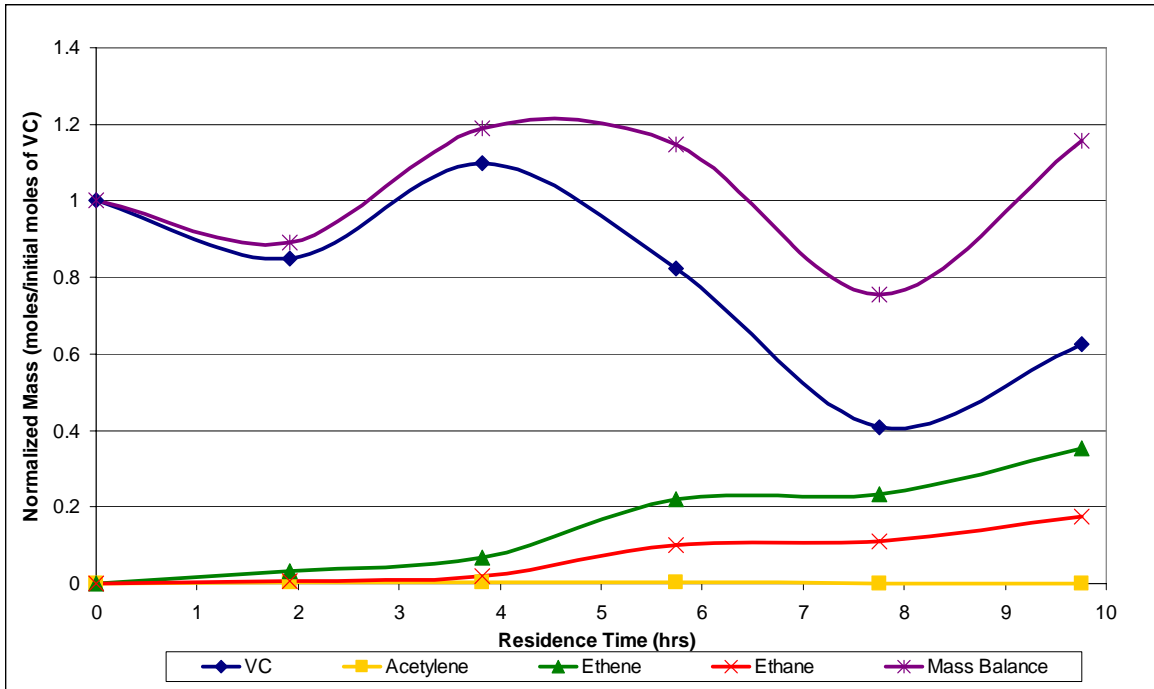
Figure 14: Degradation profiles for *cis*-DCE in columns A, B and C that were receiving three different concentrations of sulphide and 3.8-6.0 mg/L *cis*-DCE.
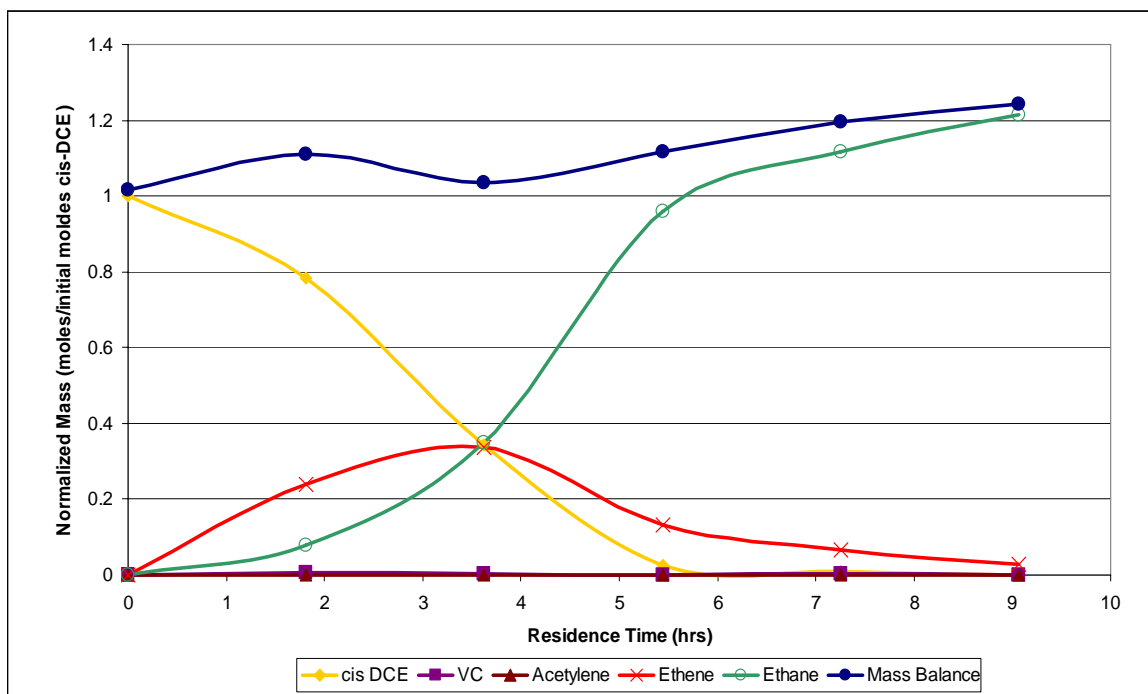
Figure 15: Typical degradation profile for *cis*-DCE in column D (Control) with an influent of 10.9 mg/L *cis*-DCE at PV 120.
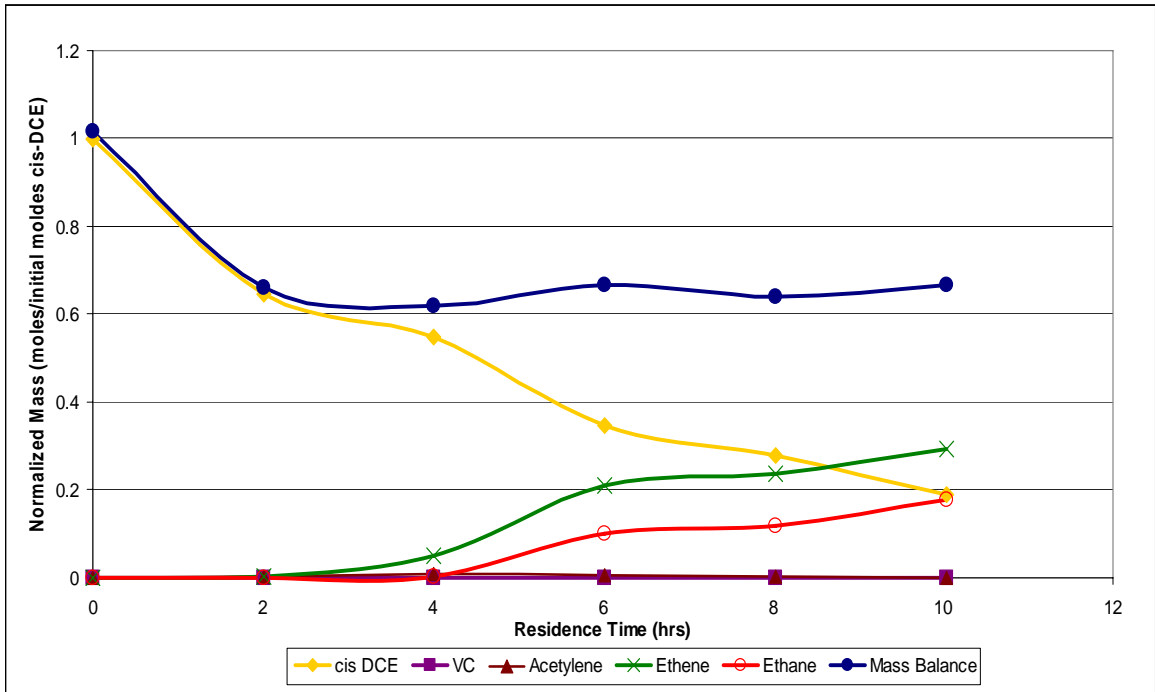
Figure 16a**:** Typical degradation profile for *cis*-DCE in the column E with an influent of 9.6 mg/L *cis*-DCE and ~7 mg/L sulphide at PV 112.
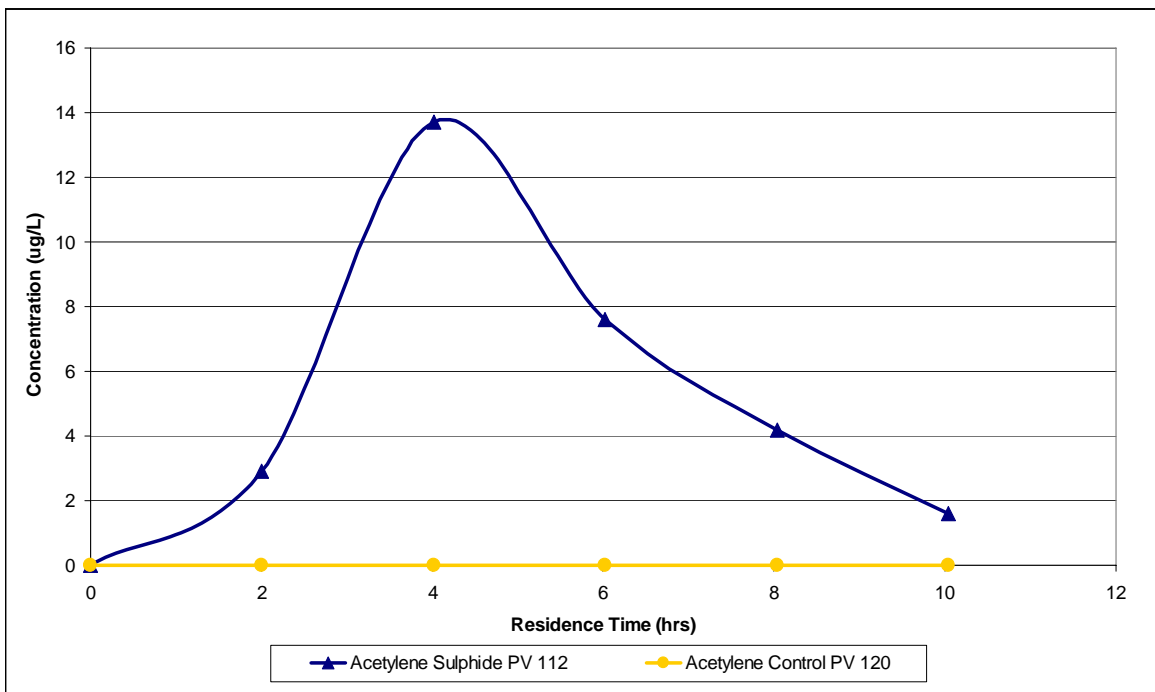
Figure 16b: Acetylene produced from the degradation of *cis*-DCE in Column D (control) and column E (7 mg/L) sulphide.
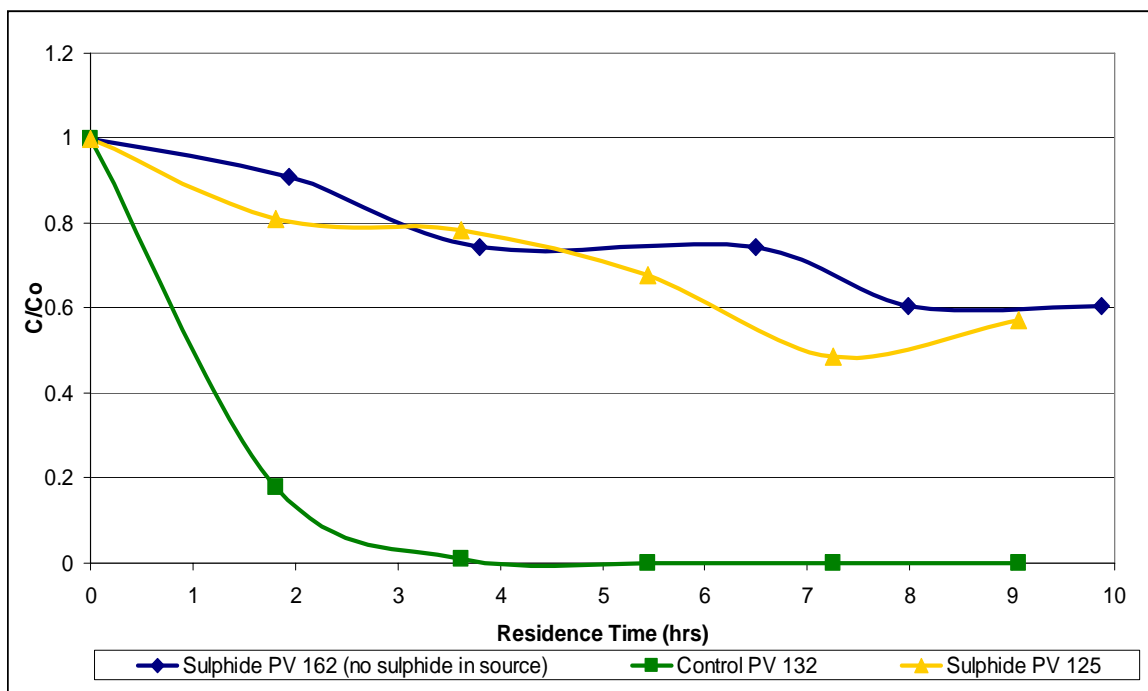
Figure 17: *cis*-DCE degradation profiles in the presence of sulphide and at 45 PV after sulphide was removed. Also shown is a profile taken at similar PV in the control column.
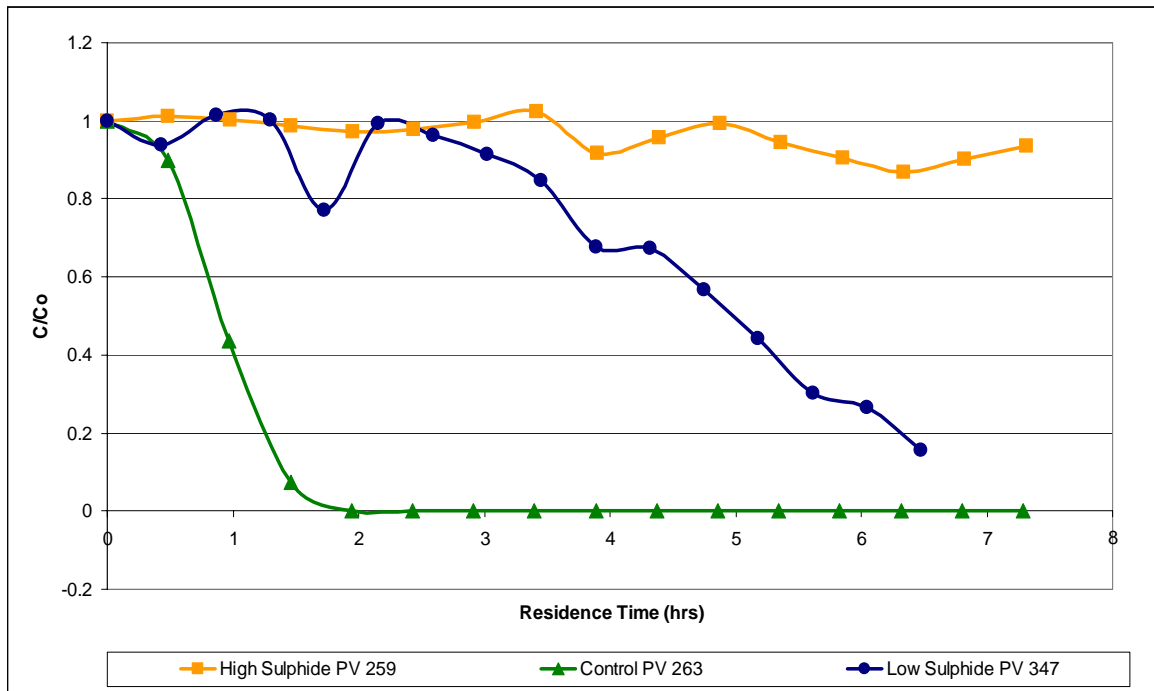
Figure 18: Degradation profiles for VC in columns A, B and C receiving three different concentrations of sulphide and ~10 mg VC.
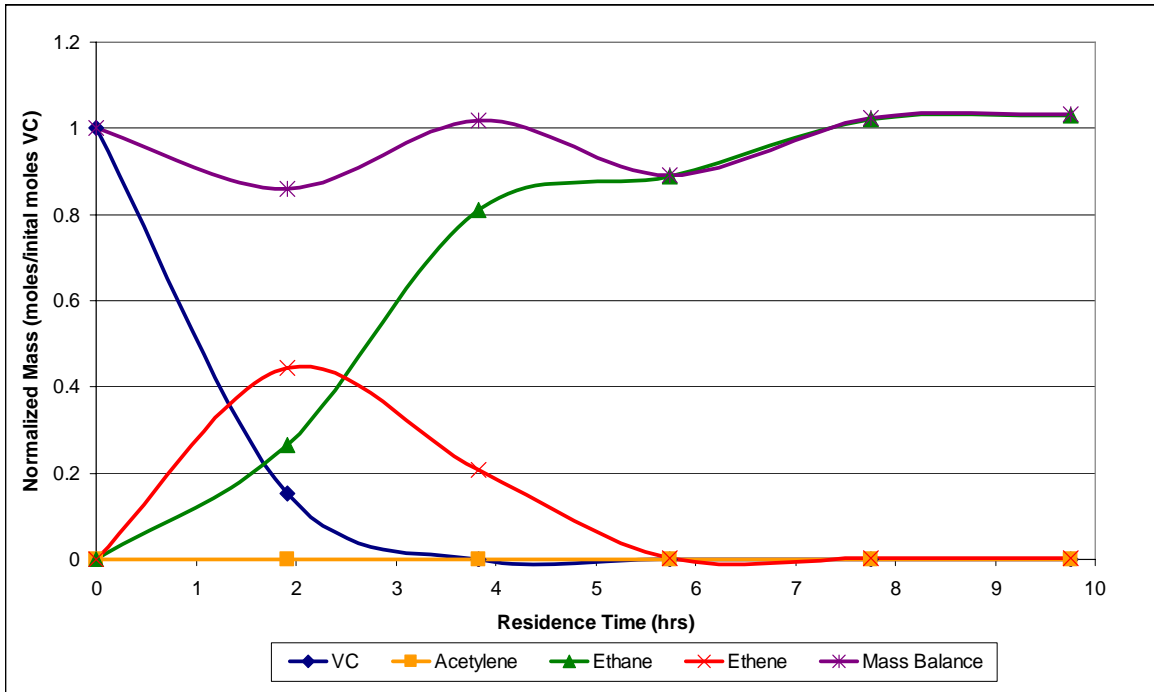
Figure 19: Degradation profile for VC in column D with an influent of 19.5 mg/L VC at PV 95.

Figure 20: Degradation profile for VC in column E with an influent of 15.4 mg/L VC and ~7 mg/L sulphide at PV 87.
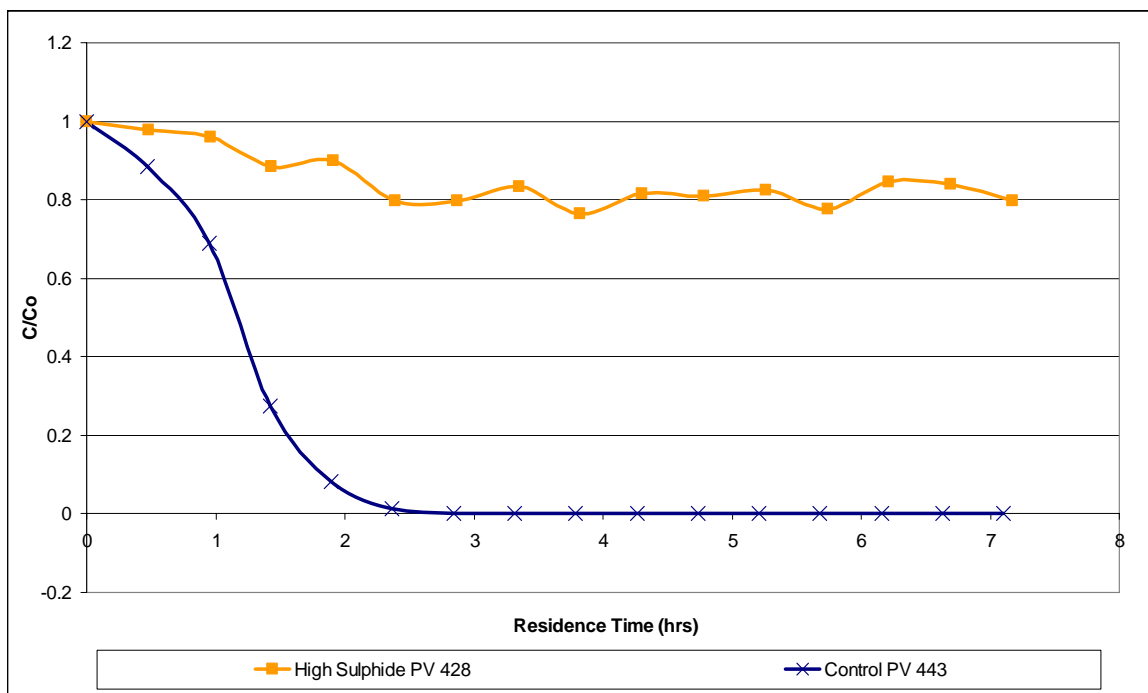
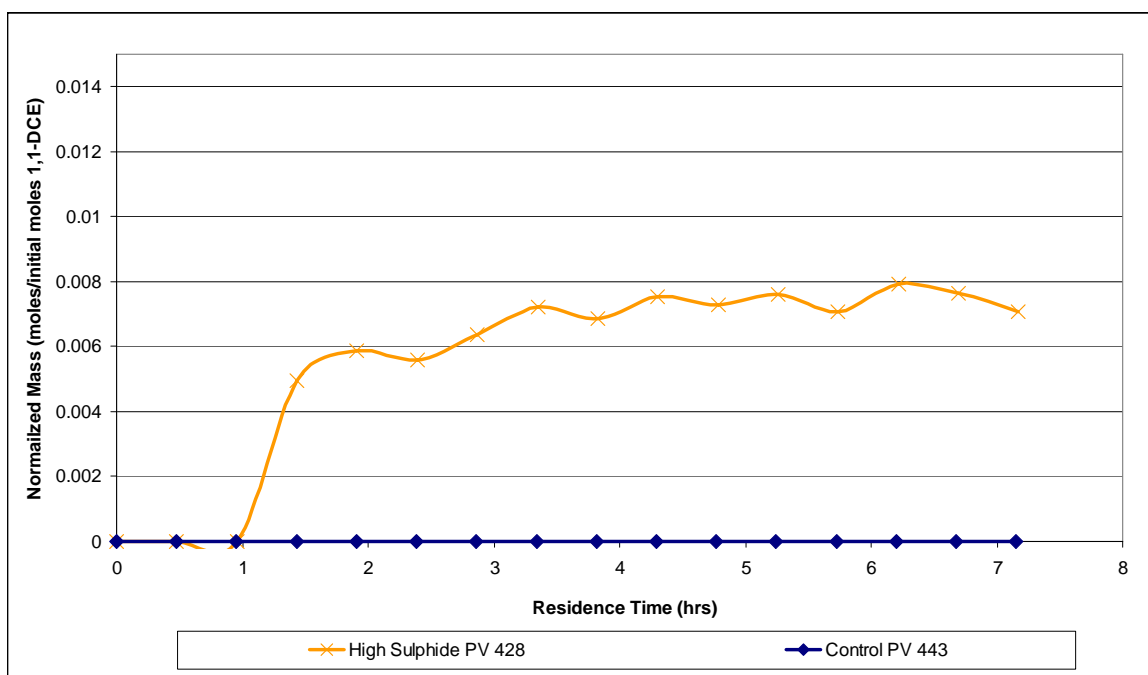Figure 21a: Degradation profiles for 1,1-DCE in columns A (Control) and C (50 mg/L sulphide) with ~10 mg/L 1,1-DCE.

Figure 21b: The production of VC from the degradation of 1,1-DCE in column A (control) and column C (~50 mg/L).
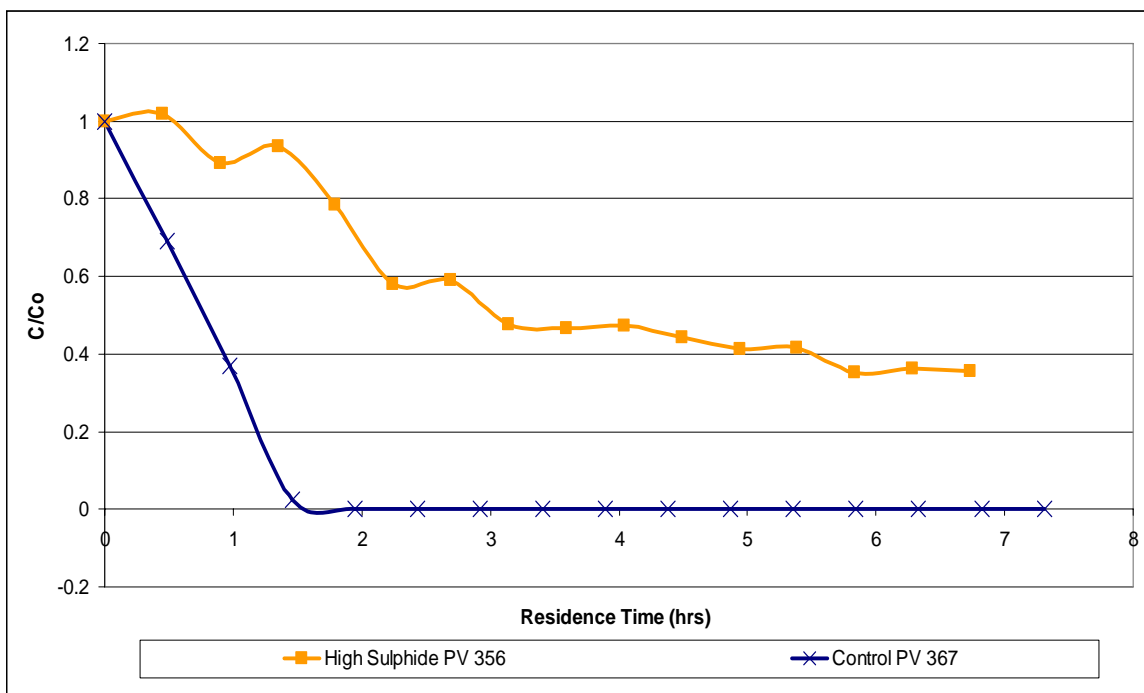
48

Figure 22a: Degradation profiles for *trans*-DCE in columns A (Control) and C (50 mg/L sulphide) with ~5 mg/L *trans*-DCE.
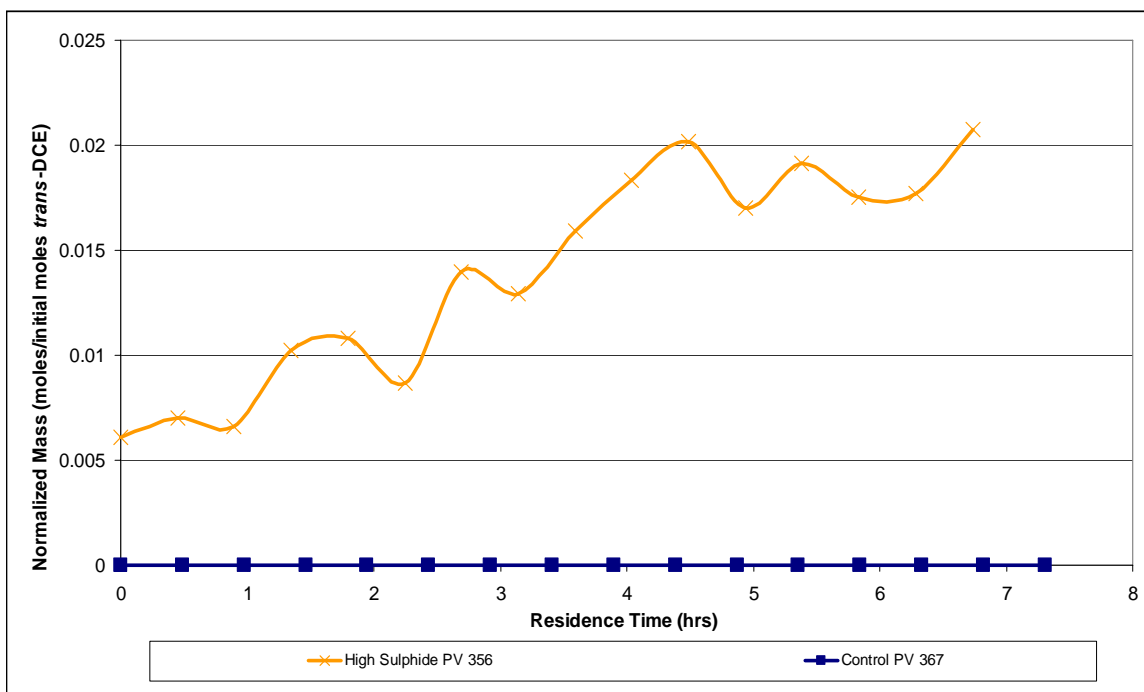

Figure 22b: The production of VC from the degradation of *trans*-DCE in column A (control) and column C (~50 mg/L).
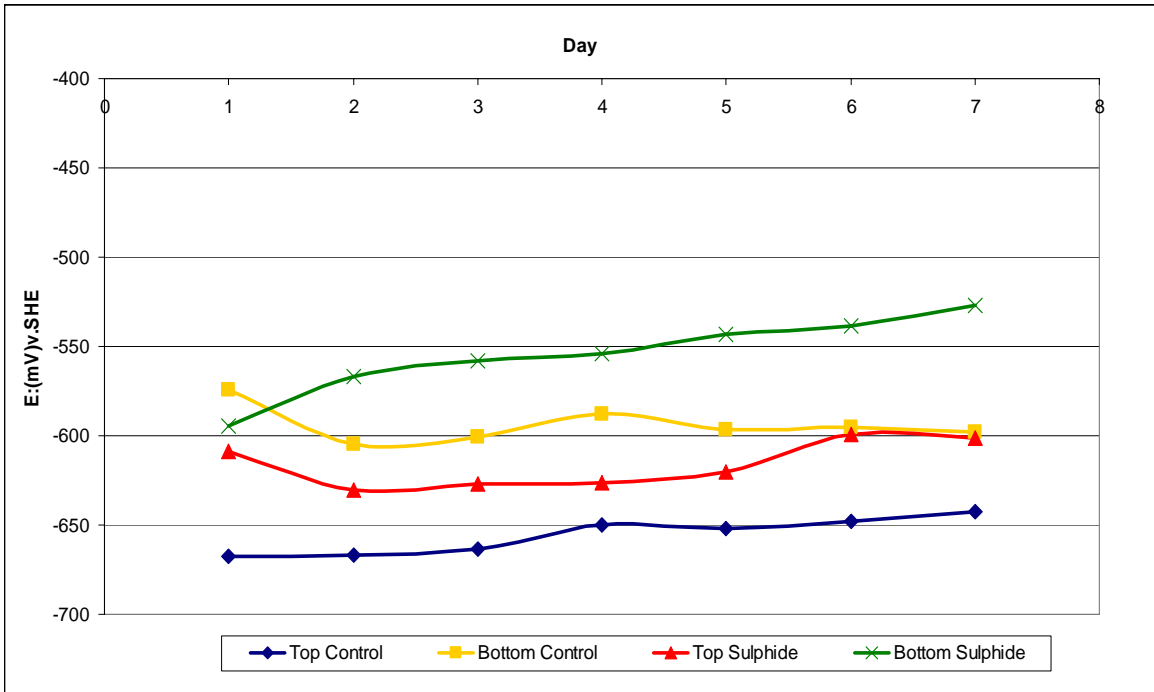
49

Figure 23: Average Corrosion Potential for TCE in columns D (Control) and E (Sulphide).
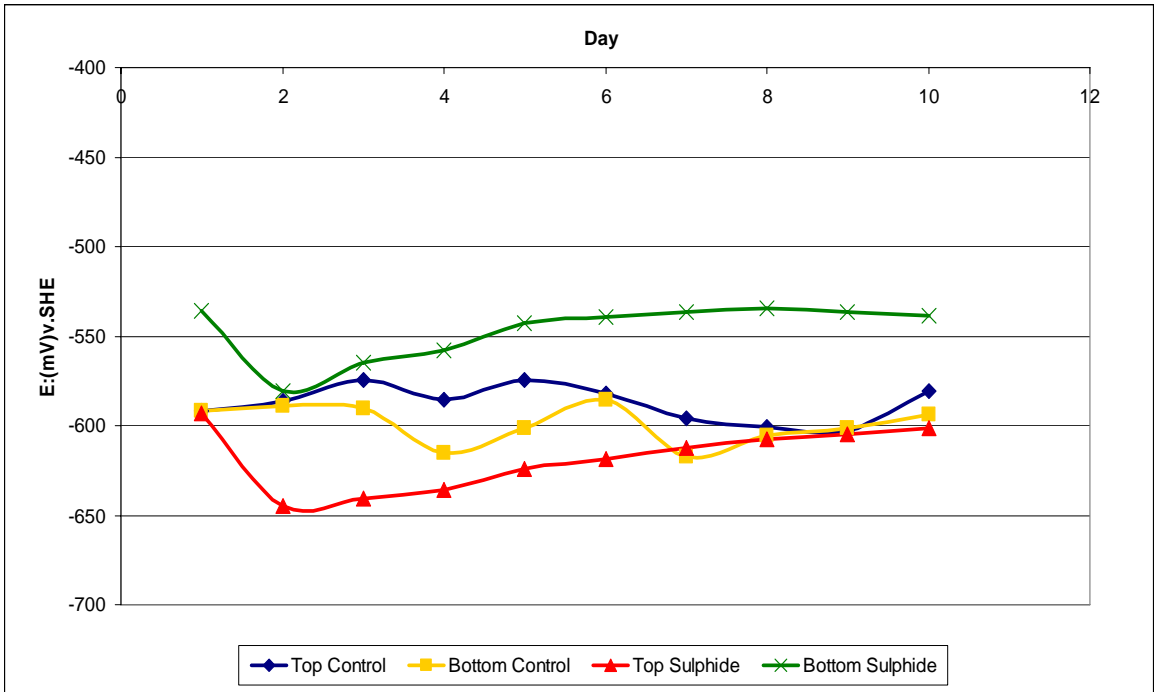

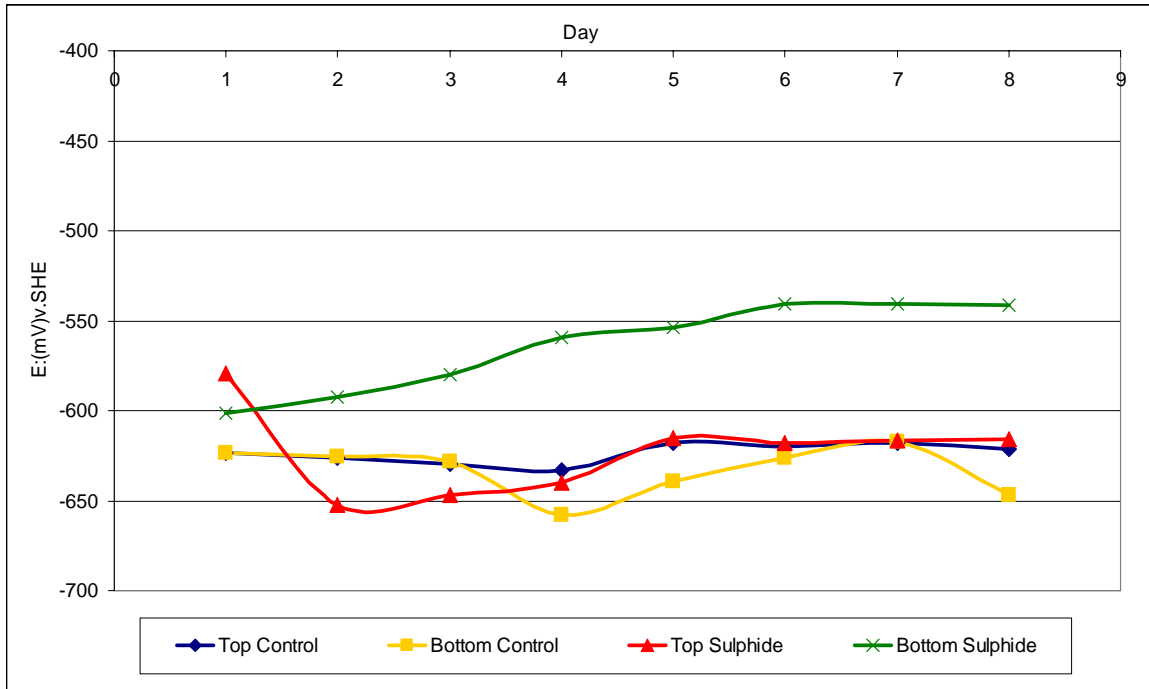Figure 24: Average Corrosion Potential for *cis*-DCE in columns D (Control) and E (Sulphide).

Figure 25: Average Corrosion Potential for VC in columns columns D (Control) and E (Sulphide).
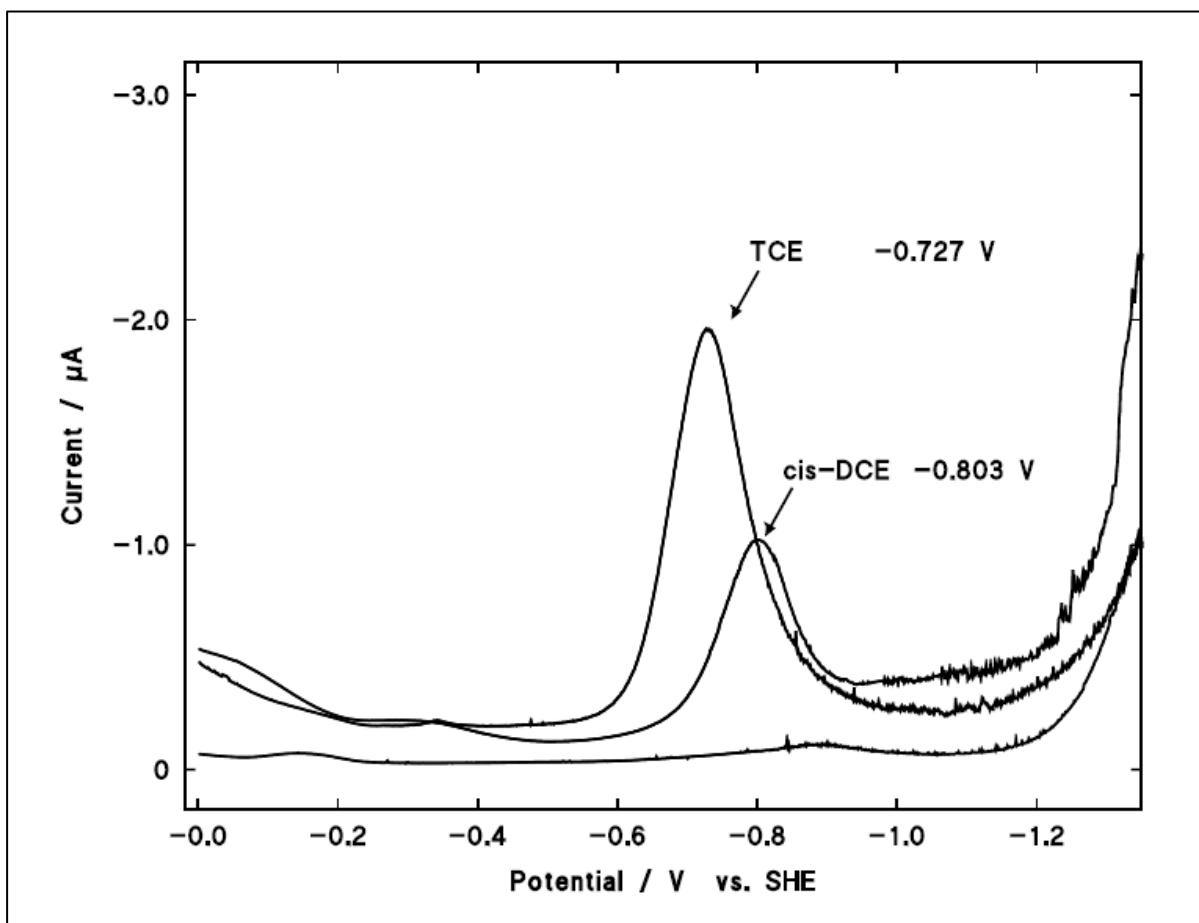
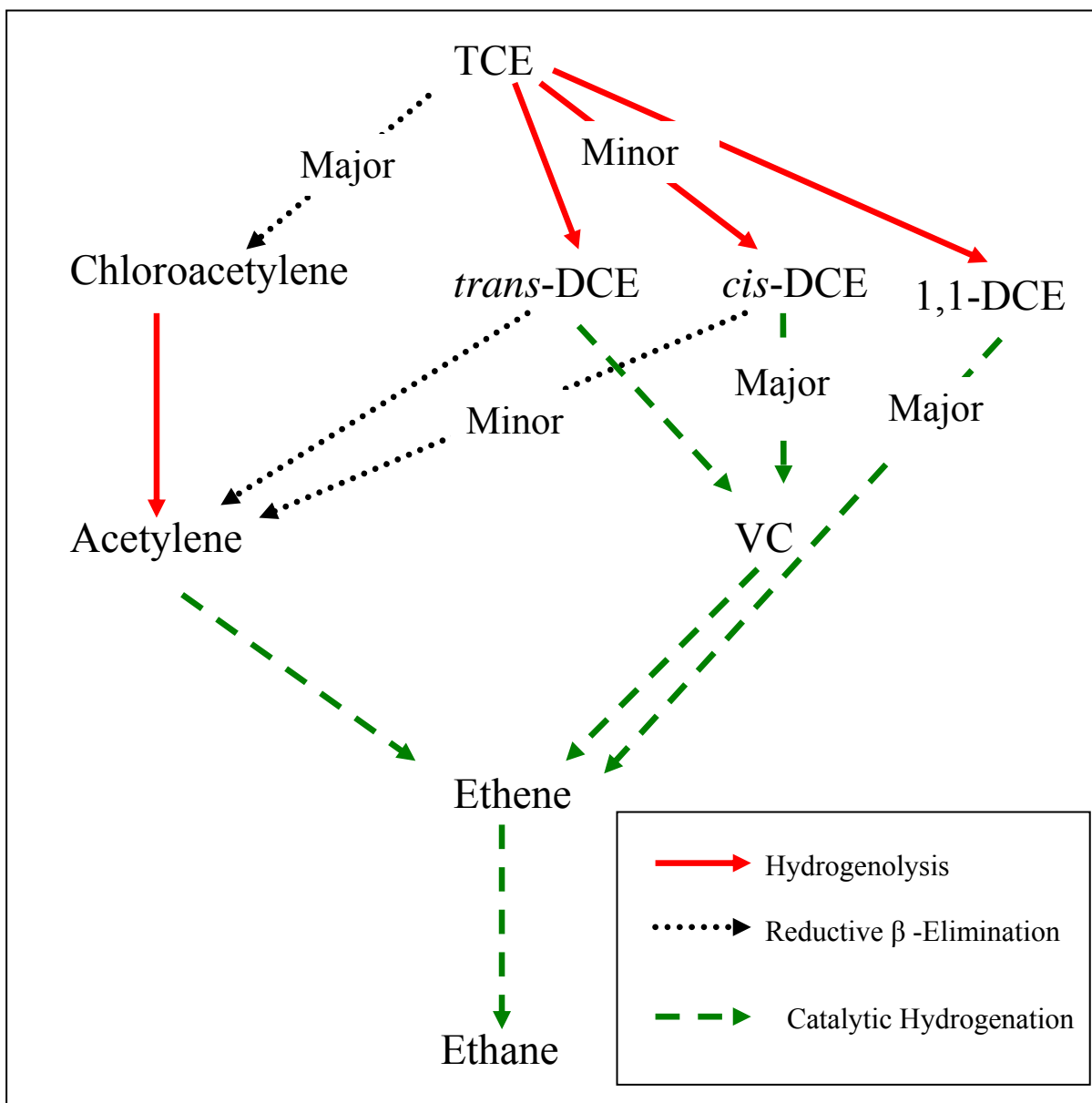Figure 26: The differential pulse voltammograms for TCE and *cis*-DCE.

Figure 27: The proposed pathways for the degradation of TCE to include the results from this study (adapted from Arnold and Roberts, 2000).

References

Arnold, W. A. and Roberts, A. L. (1998). *Pathways of chlorinated ethylene and chlorinated acetylene reaction with Zn(0)*. Environmental Science & Technology, 32, 3017-3025.

Arnold, W. A. and Roberts, A. L. (2000). *Pathways and kinetics of chlorinated ethylene and chlorinated acetylene reaction with Fe(O) particles*. Environmental Science & Technology, 34, 1794-1805.

Butler, E. C. and Hayes, K. F. (1998). *Effects of solution composition and pH on the reductive dechlorination of hexachloroethane by iron sulfide*. Environmental Science & Technology, 32, 1276-1284.

Butler, E. C. and Hayes, K. F. (1999). *Kinetics of the transformation of trichloroethylene and tetrachloroethylene by iron sulfide*. Environmental Science & Technology, 33, 2021-2027.

Butler, E. C. and Hayes, K. F. (2000). *Kinetics of the transformation of halogenated aliphatic compounds by iron sulfide*. Environmental Science & Technology, 34, 422-429.

Butler, E. C. and Hayes, K. F. (2001). *Factors influencing rates and products in the transformation of trichloroethylene by iron sulfide and iron metal*. Environmental Science & Technology, 35, 3884-3891.

Ebert, M., Kober, R., Parbs, A., Plagentz, V., Schafer, D., and Dahmke, A. (2006). *Assessing degradation rates of chlorinated ethylenes in column experiments with commercial iron materials used in permeable reactive barriers*. Environmental Science & Technology, 40, 2004-2010.

Farrell, J., Kason, M., Melitas, N., and Li, T. (2000a). *Investigation of the long-term performance of zero-valent iron for reductive dechlorination of trichloroethylene*. Environmental Science & Technology, 34, 514-521.

Farrell, J., Melitas, N., Kason, M., and Li, T. (2000b). *Electrochemical and column investigation of iron-mediated reductive dechlorination of trichloroethylene and perchloroethylene*. Environmental Science & Technology, 34, 2549-2556.

Gui, L., Gillham, R. W., and Odziemkowski, M. S. (2000). *Reduction of N-nitrosodimethylamine with granular iron and nickel enhanced iron. 1. Pathways and kinetics*. Environmental Science & Technology, 34, 3489-3494.

Klausen, J., Vikesland, P. J., Kohn, T., Burris, D. R., Ball, W. P., and Roberts, A. L. (2003). *Longevity of granular iron in groundwater treatment processes: Solution composition effects*

on reduction of organohalides and nitroaromatic compounds. Environmental Science & Technology, 37, 1208-1218.

Kober, R., Schlicker, O., Ebert, M., and Dahmke, A. (2002). *Degradation of chlorinated ethylenes by Fe-0: inhibition processes and mineral precipitation.* Environmental Geology, 41, 644-652.

Kober, R., Welter, E., Ebert, M., and Dahmke, A. (2005). *Removal of arsenic from groundwater by zerovalent iron and the role of sulfide.* Environmental Science & Technology, 39, 8038-8044.

Kohn, T., Kane, S. R., Fairbrother, D. H., and Roberts, A. L. (2003). *Investigation of the inhibitory effect of silica on the degradation of 1,1,1-trichloroethane by granular iron.* Environmental Science & Technology, 37, 5806-5812.

Kohn, T. and Roberts, A. L. (2006). *The effect of silica on the degradation of organohalides in granular iron columns.* Journal of Contaminant Hydrology, 83, 70-88.

Li, T. and Farrell, J. (2000). *Reductive dechlorination of trichloroethene and carbon tetrachloride using iron and palladized-iron cathodes.* Environmental Science & Technology, 34, 173-179.

Li, T. and Farrell, J. (2001). *Electrochemical investigation of the rate limiting mechanisms for trichloroethylene and carbon tetrachloride reduction at iron surfaces.* Abstracts of Papers of the American Chemical Society, 222, U433.

Lo, I. M. C., Lam, C. S. C., and Lai, K. C. K. (2005). *Competitive effects of trichloroethylene on Cr(VI) removal by zero-valent iron.* Journal of Environmental Engineering-Asce, 131, 1598-1606.

Matheson, L. J. and Tratnyek, P. G. (1994). *Reductive Dehalogenation of Chlorinated Methanes by Iron Metal.* Environmental Science & Technology, 28, 2045-2053.

Odziemkowski, M. S., Gui, L., and Gillham, R. W. (2000). *Reduction of N-nitrosodimethylamine with granular iron and nickel-enhanced iron. 2. Mechanistic studies.* Environmental Science & Technology, 34, 3495-3500.

Orth, W. S. and Gillham, R. W. (1996). *Dechlorination of trichloroethene in aqueous solution using Fe-O.* Environmental Science & Technology, 30, 66-71.

Phillips, D. H., Gu, B., Watson, D. B., Roh, Y., Liang, L., and Lee, S. Y. (2000). *Performance evaluation of a zerovalent iron reactive barrier: Mineralogical characteristics.* Environmental Science & Technology, 34, 4169-4176.

Ritter, K., Odziemkowski, M. S., and Gillham, R. W. (2002). *An in situ study of the role of surface films on granular iron in the permeable iron wall technology.* Journal of Contaminant Hydrology, 55, 87-111.

Ritter, K., Odziemkowski, M. S., Simpgraga, R., Gillham, R. W., and Irish, D. E. (2003). *An in situ study of the effect of nitrate on the reduction of trichloroethylene by granular iron*. Journal of Contaminant Hydrology, 65, 121-136.

Roberts, A. L., Totten, L. A., Arnold, W. A., Burris, D. R., and Campbell, T. J. (1996). *Reductive elimination of chlorinated ethylenes by zero valent metals*. Environmental Science & Technology, 30, 2654-2659.

Scherer, M. M., Richter, S., Valentine, R. L., and Alvarez, P. J. J. (2000). *Chemistry and microbiology of permeable reactive barriers for in situ groundwater clean up*. Critical Reviews in Environmental Science and Technology, 30, 363-411.

Schlicker, O., Ebert, M., Fruth, M., Weidner, M., Wust, W., and Dahmke, A. (2000). *Degradation of TCE with iron: The role of competing chromate and nitrate reduction*. Ground Water, 38, 403-409.

Tamara, M. L. and Butler, E. C. (2004). *Effects of iron purity and groundwater characteristics on rates and products in the degradation of carbon tetrachloride by iron metal*. Environmental Science & Technology, 38, 1866-1876.

Vikesland, P. J., Klausen, J., Zimmermann, H., Roberts, A. L., and Ball, W. P. (2003). *Longevity of granular iron in groundwater treatment processes: changes in solute transport properties over time*. Journal of Contaminant Hydrology, 64, 3-33.

Wust, W. F., Kober, R., Schlicker, O., and Dahmke, A. (1999). *Combined zero- and first-order kinetic model of the degradation of TCE and cis-DCE with commercial iron*. Environmental Science & Technology, 33, 4304-4309.